Preseismic electromagnetic signals in terms of complexity

K. Karamanos
Centre for Nonlinear Phenomena and Complex Systems, Université Libre de Bruxelles, Campus Plaine, C.P. 231, Boulevard du Triomphe, B-1050, Brussels

D. Dakopoulos, K. Aloupis, A. Peratzakis, L. Athanasopoulou, S. Nikolopoulos, P. Kapiris, and K. Eftaxias*
Department of Physics, Section of Solid State Physics, University of Athens, Panepistimiopolis, GR 15784 Zografos, Athens, Greece
(Received 22 July 2005; revised manuscript received 5 January 2006; published 10 July 2006)

There is a recent thesis in the literature that an important organization of a physical system precedes a catastrophic event. In this context, one can search for signatures that imply the transition from a normal state to a main catastrophic event (e.g., earthquake). Experimental techniques are thus useful in corroborating theories from observed data. For example, recent results indicate that preseismic electromagnetic time series contain information characteristic of an ensuing earthquake event. Hereby, we attempt to demonstrate that an easily computable complexity measure, such as *T*-complexity or approximate entropy, gives evidence of state changes leading to the point of global instability. The appearance of a precatastrophic state is characterized by significant lower complexity in terms of *T*-complexity and approximate entropy. The present study confirms the conclusions of previous works based on an independent linear fractal spectral analysis. This convergence between nonlinear and linear analysis provides a more reliable detection concerning the emergence of the last phase of the earthquake preparation process. More precisely, we claim that our results suggest an important principle: significant complexity decrease and accession of persistency in electromagnetic (EM) time series can be confirmed at the tail of the preseismic EM emission, which could be used as diagnostic tools for the Earth's impending crust failure. Direct laboratory and field experimental data as well as theoretical arguments support the conclusions of the present analysis.

DOI: 10.1103/PhysRevE.74.016104 PACS number(s): 91.30.Px, 05.45.Tp

I. INTRODUCTION

Recently there has been renewed interest in catastrophic events. Herein we focus on earthquakes (EQs). Fracture in heterogeneous systems has been an area of active study in recent years due to its relevance in practical engineering materials such as polycrystals and fiber composites, biological materials such as bone, and geological systems such as EQ faults [1]. We consider EQ as a large scale fracture phenomenon. The breakdown of a disordered solid is preceded by intense precursors in the form of avalanches [2]. It has been experimentally observed that the response, in terms of acoustic and electromagnetic (EM) emissions, to an increasing external stress takes place in bursts distributed over a wide range of scales; these precursors are recorded both at the laboratory and the geophysical scale [3]. In this paper, we study in terms of nonlinear and linear techniques, whether characteristic precursory signatures emerged indicating the transition to the last phases of the EQ preparation process. More precisely, first the temporal evolution of nonlinear characteristics is studied by applying a recently proposed technique: the original time EM data is projected to a symbolic sequence and then an analysis in terms of *T*-complexity follows. This analysis suggests as main result that as the nucleation phase approaches, there is a clear transition from higher to lower complexity. We verify this result in terms of a different nonlinear technique, namely, approximate entropy (APEN). Although *T*-complexity and APEN have been studied both within pure mathematics and in applications to human and animal biology, the present findings represent their first applications to preseismic EM radiations. It would be highly desirable to confirm the above-mentioned conclusion based on an independent linear fractal spectral analysis. By monitoring the temporal evolution of the fractal spectral characteristics on preseismic EM time series we show that significant alterations in associated scaling parameters occur as global failure approaches indicating a significant reduction of complexity at the tail of the preseismic EM activity, which is accompanied by the transition from antipersistent to persistent behavior. The observed convergence between nonlinear and linear analysis provides a more reliable detection concerning the emergence of the last (nucleation) phase of the EQ preparation process. Direct laboratory and field experimental data, as well as theoretical arguments, support the conclusions of the present analysis. The identification of such a transition state is of special interest for the understanding of mechanisms generating EQs.

The paper is organized as follows. In Sec. II we refer to some prerequisites. First, we present some generalities concerning EM emissions recorded prior to fracture from the laboratory to the geophysical scale and continue with data collection information. In Sec. III we present the general method, which will be applied. Section IV will be devoted to the concepts of symbolic dynamics, *T*-entropy, and approximate entropy. In Sec. V the analysis in terms of *T*-complexity and approximate entropy is applied to the preseismic EM time series. In Sec. VI the fractal spectral analysis is laid down. We then present a detailed discussion in Sec. VII. Finally in the last section we draw the main conclusions of the analysis.

*Corresponding author. Electronic address: ceftax@phys.uoa.gr

II. PREREQUISITES

A. EM emissions from fracture

Crack propagation is the basic mechanism of material's failure. The motion of a crack has been shown to be governed by a dynamical instability causing oscillations in its velocity and structure on the fracture surface. Experimental evidence indicates that the instability mechanism is that of local branching: a multicrack state is formed by repetitive, frustrated microfracturing events [4].

In many materials, emission of photons, electrons, ions, and neutral particles are observed during the formation of new surface features in fracturing, deformation, wearing, peeling, and so on. Collectively, we refer to these emissions as fractoemission [5,6]. It is worth mentioning that laboratory experiments show that more intense fractoemissions are observed during the unstable crack growth [6]. The rupture of interatomic (ionic) bonds also leads to intense charge separation that is the origin of the electric charge between the microcrack faces. On the faces of a newly created microcrack the electric charges constitute an electric dipole or a more complicated system. Due to the crack strong wall vibration in the stage of the microbranching instability, it behaves as an efficient EM emitter. The radiated EM precursors are detectable both at a laboratory [7–11] and geological scale [12–15]. Our main tool is the monitoring of the microfractures, which possibly occur in the focal area before the final breakup, by recording their EM emissions. A multidisciplinary analysis in terms of fault modeling [16], laboratory experiments [17], scaling similarities of multiple fracturing of solid materials [3], fractal electrodynamics [18], criticality [19–21], and complexity [22] seems to validate the association of the detected preseismic EM emissions with the fracturing process in the focal area of the impending EQ.

B. Data collection

Since 1994, a station was installed at a mountainous site of Zante island (37.76°N–20.76°E) in the Ionian Sea (western Greece) (Fig. 1) with the following configuration: (i) six loop antennas detecting the three components (EW, NS, and vertical) of the variations of the magnetic field at 3 and 10 kHz, respectively, (ii) two vertical $\lambda/2$ electric dipoles detecting the electric-field variations at 41 and 54 MHz, respectively, and (iii) two short thin wire antennas (STWA) of 100 m length each, lying on the Earth's surface, detecting ultralow frequency (ULF) (<1 Hz) anomalies, at EW and NS direction, respectively. The 3, 10, 41, and 54 MHz were selected in order to minimize the effects of the sources of manmade noise in the mountain area of the Zante island. All the EM time series were sampled at 1 Hz. Such an experimental setup helps to specify not only whether or not a single EM anomaly is preseismic in itself, but also whether a combination of such disturbances at different frequencies could be characterized as preseismic. In this work, we focus on the precursory EM emissions associated with the Kozani-Grevena (KG) and Athens EQs, because they have a rather long duration, thus it provides sufficient data for statistical analysis (see the remark at the end of this section).

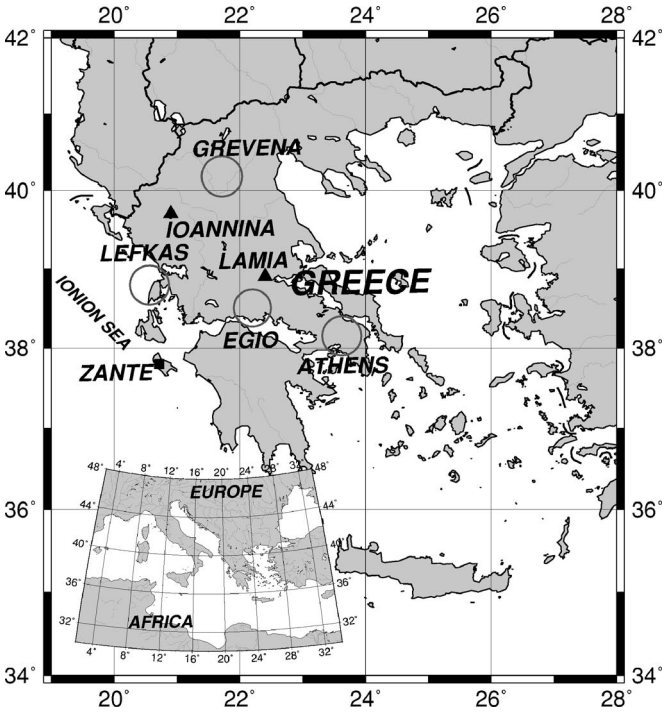

FIG. 1. A map demonstrating (i) the location of the Zante experimental station recording kHz and MHz EM disturbances, and (ii) the location of the Lamia station recording ultralow-frequency (<1 Hz) geoelectric signals. The circles indicate the epicenters of the Athens, Kozani-Grevena, Egio-Eratini, and Lefkas EQs.

C. EM anomalies prior to the Athens earthquake

On September 7, 1999 at 11:56 GMT the Athens EQ (38.2°N,23.6°E) with a magnitude M_w=5.9 occurred (Fig. 1). Clear EM anomalies at 3 and 10 kHz had been simultaneously recorded during the last few days prior to this EQ [16,19,23]. Figure 2 shows the anomaly recorded at 3 kHz (E-W) magnetic loop antenna. They are characterized by an accelerated emission rate, while these radiations are embedded in a long duration quiescence period. Weak anomalies were also simultaneously recorded at 41, 54, and 135 MHz on 29 August 1999 (see Fig. 6 in Ref. [19]). The kHz precursory emissions have a rather unanticipated long duration,

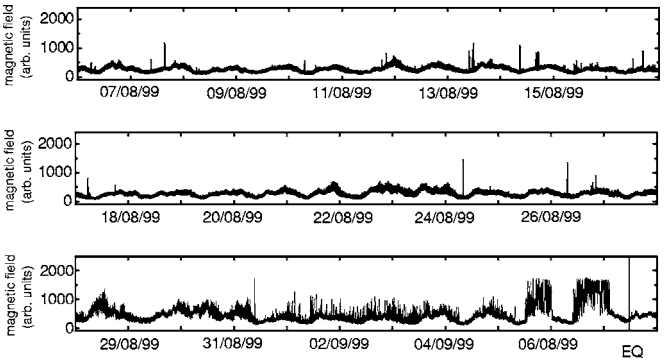

FIG. 2. EM anomalies detected at 3 kHz (E-W) loop antenna preceding the M_s=5.9 Athens EQ. The *y* axis shows the output in mV of the receiver.

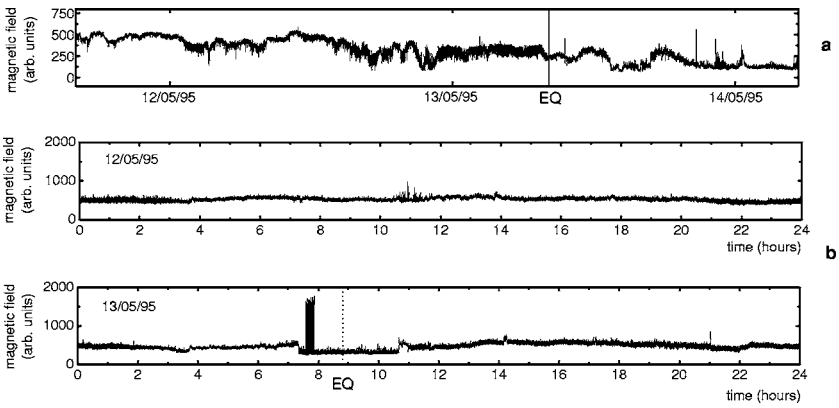

FIG. 3. EM anomalies detected at (a) 41-MHz dipole $\lambda/2$ antenna and (b) 3-kHz (vertical) loop antenna preceding the Kozani-Grevena EQ. The y axis shows the output in mV of the receivers.

while the sampling rate was 1 sample/sec, and thus they provide sufficient data for statistical analysis. The seismogenic origin of these EM activities have been supported by a series of previous papers [3,16,18–20,22,23].

D. EM anomalies prior to the Kozani-Grevena earthquake

On May 13, 1995 the Kozani-Grevena (KG) EQ occurred in NW Greece (40.2°N,21.7°E) with a magnitude M_w =6.6 (Fig. 1). kHz-MHz EM anomalies had been observed before this EQ in Zante station with the following order (Fig. 3): (i) A few tens of hours before the main event, EM anomalies were simultaneously recorded at 41 and 54 MHz, with increasing EM emission rate [17]. These anomalies ceased approximately one hour before the EQ occurrence. Figure 3(a) shows the 41-MHz EM time-series recorded during the last tenths of hours before the KG EQ. (ii) Very strong multipeaked EM signals, with sharp onsets and ends, at 3 and 10 kHz, lasting about a half hour, were simultaneously emerged approximately one and a half hours before the main event. Figure 3(b) shows the EM time series recorded by the 3-KHz (vertical) loop antenna. We draw attention to the almost simultaneous cessation of these EM anomalies at both (kHz and MHz) frequency bands although they had very different onset times. The possible seismogenic origin of these EM activities has also been supported by a series of previous papers [17–21]. (iii) An ultralow frequency (<1 Hz) preseismic EM anomaly was recorded in the STWA sensors [18] (Fig. 4). If someone follows the daily background pattern of the ULF recordings one finds the existence of a minimum around mid-day. However, as the EQ approaches this behavior changes and a maximum instead of a minimum now is seen one day before the EQ. The curve attains its normal shape a few days after the event [3,18]. There is a growing number of indications on possible coupling between ionospheric anomalies and EQs [3]. The behavior of this anomaly supports the hypothesis of a relationship between thermodynamic processes produced by increasing tectonic stresses in the Earth's crust and attendant EM interactions between the crust and ionosphere [13,14,18]. The appearance of the former ULF anomaly verifies that the fractoelectrification, and thus the fracture process, has been extended up to the surface layer of the crust.

E. Geomagnetic activities during the detected precursory EM emissions

A serious problem in the study of seismogenic emissions is the distinction from noise of the emissions possibly associated with EQs. There are emissions originated in the ionosphere and magnetosphere, which are found to be closely related to geomagnetic activities. We focus on this point. The geomagnetic activity, as expressed by the planetary 3-h-range Kp index (http://www.gfz-potsdam.de/pub/home/obs/kp-ap/), is depicted in the visualization of the Kp values utilizing the Bartels musical diagram (Fig. 5). Based on the classification of days, deduced from Kp indices, one can rec-

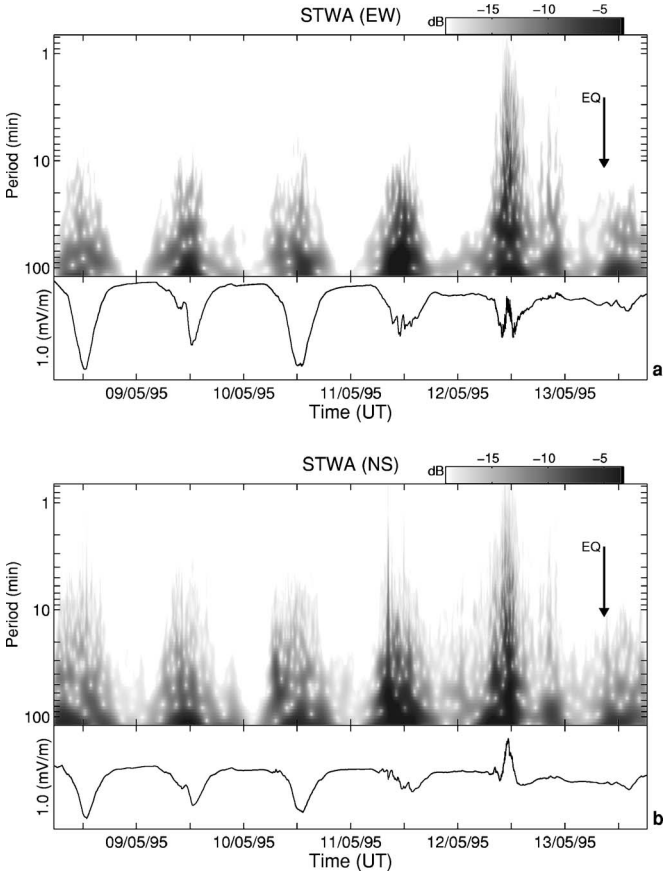

FIG. 4. The wavelet power spectrum of the ultra low frequency (<1 Hz) electric anomaly recorded on 12 May 1995 (see text) by the short thin wire antennas (STWA) (upper part) along with their corresponding time series (lower part) at (a) east-west STWA antenna; (b) north-south STWA antenna. The intensity scale on the top of each diagram corresponds to the values of the square spectral amplitudes, in arbitrary units. The spectra reveal an accelerating energy release as the main shock approaches.

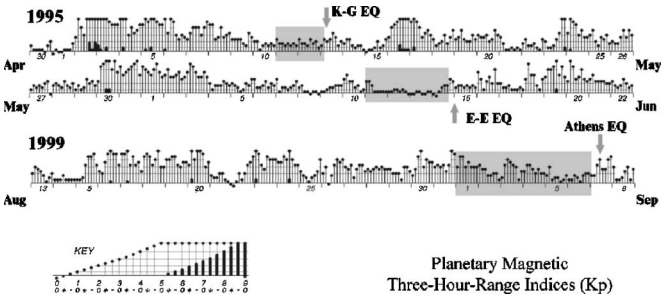

FIG. 5. The temporal evolution of the geomagnetic activity as expressed by the planetary 3-h-range Kp index (http://www.gfz-potsdam.de/pub/home/obs/kp-ap/). The shaded frames indicate the time windows of the precursory EM activities recorded before the Kozani-Grevena, Egio-Eratini, and Athens EQs. One can recognize that the precursory EM phenomena have been detected during low geomagnetic activity.

ognize that the recorded sequence of EM emissions before the Kozani-Grevena, Egio-Eratini (EE), and Athens EQs were observed during quiet magnetic conditions. We have also investigated the meteorological activity indicating that it is unlikely that the observed anomaly have any relation to meteorological effects. The above information supports the hypothesis that the recorded precursory EM radiations, which are embedded in a long duration quiescence period concerning the detection of EM disturbances at 3 kHz, 10 kHz, 41 MHz, and 54 MHz, could be related to the fracture activity during the EQ preparation process.

Remark: It would be desirable to have the possibility to analyze more preseismic EM emissions. However, we stress that in order to be possible to extract useful information concerning the preparation of the last stages of the EQ process, the associated EM precursors must satisfy the following requirements. (i) It must have a long duration, that is, from a few tens of hours up to a few days, in order to contain the relevant information. Additionally, a long duration is required in order to use the measurements for statistical purposes. (ii) The recorded radiation must be emerging clearly from the EM background. This means that the detected EM radiation has not been significantly absorbed by conducting layers of the crust or the even more conductive sea, implying that useful EM precursor must be associated with an on-land seismic event which is both strong, i.e., with magnitude ~6 or greater, and shallow. In this case we have reasons to assert that the fracture process is extended up to the surface layer of the crust, and thus the captured precursory kHz, MHz EM emissions are produced by a population of EM emitters (opening cracks) that is sufficient to represent the behavior of the total number of the activated cracks during the evolution of fracture. The absence in many cases of clear precursory emissions, in particular in the MHz frequency band, becomes understandable. However, such strong surface EQs that occur on land are not so common events in a given region like Greece; the majority of EQs with magnitude greater or equal to 6 occur in the sea. During the period of function of our experimental station, i.e., during the last ten years, only two strong surface EQs occurred in the continental Greece, namely, the May 13, 1995, Kozani-Grevena EQ and the September 7, 1999, Athens EQ. An outstanding feature of the KG EQ was the clearly observed extended surface fault traces [17], while in the case of the Athens EQ the energy centroid depth was 10.3 km for the main fault, and 5.4 km for the secondary one [23]. We recall that the EQ focal dimension L is related with the EQ magnitude M, through the empirical equation suggested by Kanamori and Anderson [57]: $\log_{10}L=0.5M-1.9$.

We systematically receive candidate precursory kHz signals for EQs with magnitude greater or equal to 6 that take place close to coastline. However, in this case, due to absorption, we receive only the most intense EM pulses. Hence the precursory signals have a strong intermittent structure and relatively short duration. These characteristics do not allow the application of the methods presented here (from the arsenal of statistical physics) to their study. In the sequel we present two such characteristic candidate preseismic disturbances.

On 15 June 1995, a strong ($M_w=6.6$) seismic event (Egio-Eratini EQ) occurred near the coastline of the Corinthian Gulf at 00:15:51.0 UTC (Fig. 1). According to the calculations of the USGS the epicenter was on the side of the land, while, according to the calculation of the National Observatory of Athens the epicenter laid on the side of the sea. For this EQ we had precursory EM emissions, namely, (i) weak MHz anomalies, and (ii) strongly sporadic kHz anomalies of short duration. Figure 6(a) depicts the output of the 3-kHz (vertical) loop antenna.

On 14 August 2003 at 05:14: 53.9 UTC an EQ of $M_w=5.9$ occurred near the coastline of Lefkas Island in the Ionian Sea (Fig. 1). Before this EQ, namely on 13 August 2003, clear intermittent EM anomalies were simultaneously detected at both the 3- and 10-kHz magnetic loop antennas

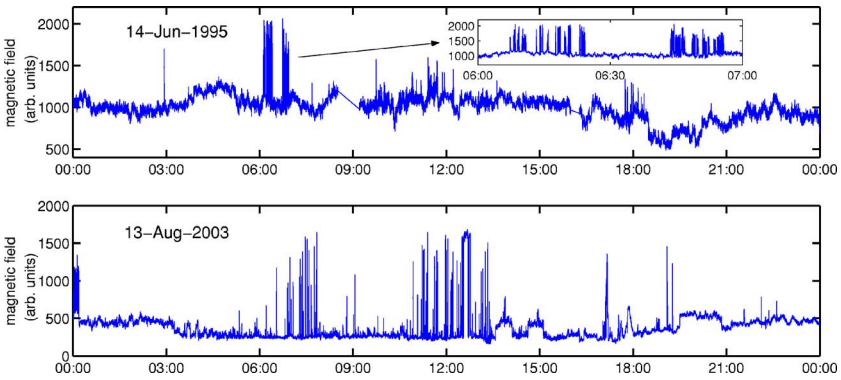

FIG. 6. (Color online) EM anomalies detected at 3-kHz (vertical) loop antenna preceding (a) the ($M_w=6.6$) Egio-Eratini EQ on 15 June 1995, at 00:15:51.0 UTC (Fig. 1), and (b) ($M_w=5.9$) Lefkas EQ on 14 August 2003 at 05:14: 53.9 UTC (Fig. 1). The y axis shows the output in mV of the receiver.

(EW, NS, and vertical). These anomalies have duration of a few hours and are also embedded in a quiescence period concerning the detection of EM disturbances at 3 and 10 kHz. Figure 6(b) depicts the output from the 3-kHz (vertical) loop antenna.

The potential seismogenic origin of the above-mentioned signals is only based on empirical arguments and thus we consider the emissions of this category as hypothetical precursory EM phenomena.

III. GENERAL METHOD

A way to examine transient phenomena is to divide the measurements into time windows of small duration and analyze them. If this analysis yields different results for some precursory epochs, then a transient behavior can be extracted.

Herein, dividing the whole preseismic EM time series into successive time windows of short duration, i.e., each one of 1024 sample points (seconds), we calculate the T-entropy, the approximate entropy, and the Hurst exponent of the fractal spectral analysis, associated with the successive time windows we created. First, we focus on the temporal evolution of T-entropy. If the analysis yields different T-entropy values for a big enough population of time windows, then a distinctive preseismic epoch in the time series, probably corresponding to a characteristic stage of the preparation process of the EQ event, can be recognized. In other words, the appearance of a different new epoch is understood as an ensemble of time windows with short duration having different T-entropy values. Thus, based on the temporal evolution of T-complexity values, we try to recognize distinct epochs for the generation of the catastrophic event. We repeat the same procedure studying the time series in terms of approximate entropy, as well as in terms of the spectral fractal analysis, focusing on the emergence of distinctive epochs. We examine if the different epochs defined by the T-complexity, approximate entropy, and Hurst exponent, coincide in their results. This indeed is happening, since the epochs obtained by the first two kinds of nonlinear analysis are exactly the same to those obtained by the method of fractal spectral analysis. The fundamental purpose of this work is to relate the extracted different precursory epochs with different stages of the EQ preparation process. Finally, we examine whether laboratory and field measurements, as well as theoretical arguments, justify the documented different epochs and stages of EQ preparation process.

IV. THE CONCEPTS OF T-COMPLEXITY AND APPROXIMATE ENTROPY

A. Symbolic dynamics

The discovery that simple deterministic systems can show a vast diversity of behavior in response to variations of initial conditions and/or control parameters has been at the origin of an intense interdisciplinary research activity during the last two decades [24–26]. One of the outcomes of this work has been the realization that for an appropriate description of such complex systems, one needs to resort to a probabilistic approach [27]. Now, once one leaves the description in terms of trajectories, a basic question that must be dealt with concerns the amount of information one may have access to on the evolution of the system in the course of time.

One of the approaches developed in this context is *coarse graining*, whereby a complex system is viewed as an *information generator* producing messages constituted of a discrete set of symbols defined by partitioning the full continuous phase space into a finite number of cells. We refer to such a description as "symbolic dynamics" [25–28]. One of its merits is to provide a strong link between dynamical systems and information theory [25,29,30].

From the initial dynamical system we can generate a sequence of symbols, where the dynamics of the original (under analysis) system has been projected. This symbolic sequence can be analyzed by terms of information theory such as entropy estimations, information loss, automaticity, and other prominent properties.

There exist some canonical ways for generating symbolic dynamics out of a given dynamical system [25,26,28,29,31]. To produce symbolic dynamics out of the evolution of a given system, we set up a coarse-grained description incorporating from the very beginning the idea that a physically accessible state corresponds to a finite region rather than to a single point of phase space. Let S_i $(i=1,2,\ldots,K)$ be the set of cells in phase space constituted by these regions, assumed to be connected and nonoverlapping. As time goes on, the phase-space trajectory performs transitions between cells thereby generating sequences of K symbols, which may be regarded as the letters of an alphabet. We shall require that, in the course of these transitions, each element of the partition is mapped by the law of evolution on a union of elements.

In this paper we first restrict ourselves to the simplest possible coarse graining of the preseismic signal. This is given by choosing a threshold C and assigning the symbols "1" and "0" to the signal, depending on whether it is above or below the threshold (binary partition). In this way, each time window of the original EM time series for a given threshold is transformed into symbolic sequences, which contains "linguistic" or "symbolic dynamics" characteristics. The selection of a two-symbol alphabet satisfies terms of simplicity and computational convenience. Last, we also study the cases of more than two symbols alphabets (Fig. 12). We conclude with similar results.

B. T entropy

In this section we introduce the grammar-based complexity measure referred to here as the T-entropy. T-entropy is a different grammar-based complexity and information measure defined for infinite, as well as finite, strings of symbols [32,33]. It is a weighted count of the number of production steps required to construct the string from its alphabet. Briefly, it is based on the intellectual economy one makes when rewriting a string according to some rules. The basic fact for the T-complexity is that it puts the problem of the algorithmic compressibility in a well understandable basis (and also in a firm mathematical basis).

Let us note again that the method of T-entropy is based in the *rewriting* of a word according to some basic rules. This way of rewriting is unique and therefore leads to a unique characterization by the corresponding T-complexity measure. Before analyzing in some depth the results coming from the application of the notion of T-complexity in real-world problems, we would like to describe how the T-complexity is computed, at least for finite strings.

The *T-complexity* of a string is defined by the use of one *recursive hierarchical pattern copying (RHPC) algorithm*. It computes the *effective number of T-augmentation steps* required to generate the string.

The T-complexity may be thus computed effectively from any string and the resultant value is unique.

The string $x(n)$ is parsed to derive constituent patterns $p_i \in A^+$ and associated copy exponents $k_i \in N^+$, $i=1,2,\ldots,q$, where $q \in N^+$ satisfying

$$x = p_q^{k_q} p_{q-1}^{k_{q-1}} \cdots p_i^{k_i} \cdots p_1^{k_1} \alpha_0, \quad \alpha_0 \in A. \tag{1}$$

Each pattern p_i is further constrained to satisfy

$$p_i = p_{i-1}^{m_{i,i-1}} p_{i-2}^{m_{i,i-2}} \cdots p_j^{m_{i,j}} \cdots p_1^{m_{i,1}} \alpha_i,$$

$$\alpha_i \in A \quad \text{and} \quad 0 \le m_{i,j} \le k_j. \tag{2}$$

The *T-complexity* $C_T(x(n))$ is defined in terms of the copy exponents k_i:

$$C_T(x(n)) = \sum_i^q \ln(k_i + 1). \tag{3}$$

One may verify that $C_T(x(n))$ is minimal for a string comprising a single repeating character. From Eq. (3) we have

$$\ln n \le C_T(x(n)). \tag{4}$$

The upper bound is more difficult to derive. However, for $n > n_0$

$$C_T(x(n)) \le \mathrm{li}(\ln 2 \ln(\#A^n)), \tag{5}$$

where $\mathrm{li}(z) = \int_z^0 du/\ln u$ is the logarithmic integral function. For a binary alphabet $n_0 \simeq 15$, i.e., small enough to be of no consequence as we are typically concerned with strings in the range of $n = 10^4 - 10^6$ bits. In practice we parse the string repeatedly from *left to right* but select the *patterns from right to left*.

The *T-information* $I_T(x(n))$ of the string $x(n)$ is defined as the *inverse logarithmic integral* of the T-complexity divided by a scaling constant $\ln 2$:

$$I_T(x(n)) = \mathrm{li}^{-1}\left(\frac{C_T(x(n))}{\ln 2}\right). \tag{6}$$

In the limit $n \to \infty$ we have that $I_T(x(n)) \le \ln(\#A^n)$. The form of the right-hand side may be recognizable as the maximum possible n-block entropy of Shannon's definition. The neperian logarithm implicitly gives to the T-information the units of nats. $I_T(x(n))$ is the total T-information for $x(n)$. The *average T-information rate per symbol*, referred to here as the average T-entropy of $x(n)$ and denoted by $h_T(x(n))$, is defined along similar lines,

$$h_T(x(n)) = \frac{I_T(x(n))}{n} (\text{nats/symbol}). \tag{7}$$

Clearly we note that in the limit of $n \to \infty$, $h_T(x(n)) \le \ln(\#A) = K$. The correspondence between the T-information and T-entropy on the one hand and Shannon's entropy definitions on the other hand is reinforced in subsequent investigations [32]. An example of an actual calculation of the T-complexity for a finite string is given in Ref. [32].

C. Approximate entropy

Related to time series analysis, APEN provides a measure of the degree of irregularity or randomness within a series of data (of length N). APEN was pioneered by Pincus as a measure of system complexity [34]. It is closely related to Kolmogorov entropy, which is a measure of the rate of generation of new information. This family of statistics is rooted in the work of Grassberger and Procaccia [35] and has been widely applied in biological systems (Ref. [36] and references therein).

The approximate entropy examines time series for similar epochs: more similar and more frequent epochs lead to lower values of APEN. In a more qualitative point of view, given N points, the APEN-like statistics is approximately equal to the negative logarithm of the conditional probability that two sequences that are similar for m points remain similar, that is, within a tolerance r, at the next point. Smaller APEN values indicate a greater chance that a set of data will be followed by similar data (regularity), thus smaller values indicate greater regularity. Conversely, a greater value for APEN signifies a lesser chance of similar data being repeated (irregularity), hence greater values convey more disorder, randomness, and system complexity. Thus a low or high value of APEN reflects a high or low degree of regularity. The following is a description of the calculation of APEN. Given any sequence of data points $u(i)$ from $i = 1 to N$, it is possible to define vector sequences $x(i)$, which consist of length m and are made up of consecutive $u(i)$, specifically defined by the following:

$$x(i) = (u[i], u[i+1], \ldots, u[i+m-1]). \tag{8}$$

In order to estimate the frequency that vectors $x(i)$ repeat themselves throughout the data set within a tolerance r, the distance $d(x[i], x[j])$ is defined as the maximum difference between the scalar components $x(i)$ and $x(j)$. Explicitly, two vectors $x(i)$ and $x(j)$ are "similar" within the tolerance or filter r, namely $d(x[i], x[j]) \le r$, if the difference between any two values for $u(i)$ and $u(j)$ within runs of length m are less than r [i.e., $|u(i+k) - u(j+k)| \le r$ for $0 \le k \le m$]. Subsequently, $C_i^m(r)$ is defined as the frequency of occurrence of similar runs m within the tolerance r:

$$C_i^m(r) = [\text{number of } j \text{ such that } d(x[i], x[j]) \le r]/(N - m - 1), \text{ where } j \le (N - m - 1).$$

Taking the natural logarithm of $C_i^m(r)$, $\Phi^m(r)$ is defined as the average of $\ln(C_i^m(r))$:

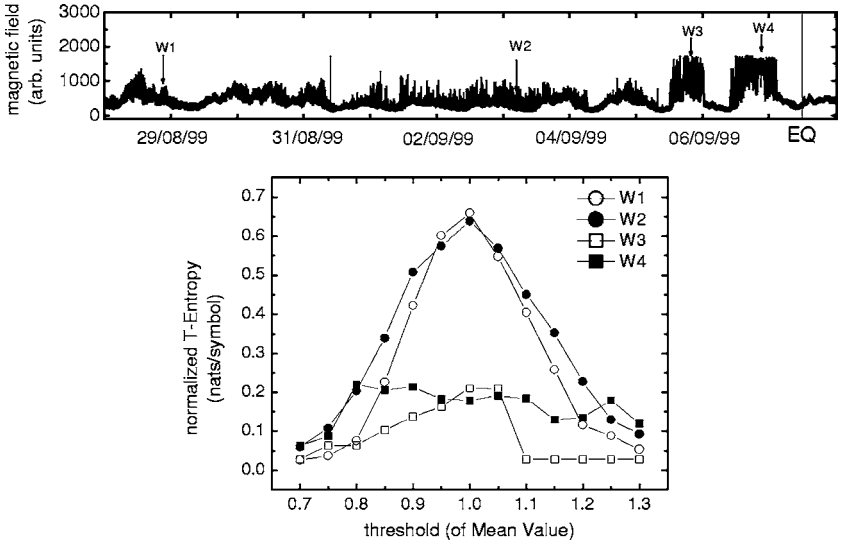

FIG. 7. The W_i in the upper panel are windows of 1024 elements each one. The bottom panel refers to the choice of the optimal partition for these windows. First, the normalized pseudo-T-entropy is computed for different partitions. To obtain these partitions, we change the value of the threshold C by 0.05 of the mean value, from 0.7 of the mean value to 1.3 of the mean value. The normalized T-entropy corresponds to the optimal partition, which is obtained by the maximization of the pseudo-T-entropy (see text). We observe that it can be considered, without a significant error, that the optimal partition corresponds to the mean value.

$$\Phi^m(r) = \sum_i \ln C_i^m(r)/(N-m-1), \tag{9}$$

where Σ_i is a sum from $i=1$ to $(N-m-1)$. $\Phi^m(r)$ is a measure of the prevalence of repetitive patterns of length m within the filter r.

Finally, approximate entropy, or APEN(m,r,N), is defined as the natural logarithm of the relative prevalence of repetitive patterns of length m as compared with those of length $m+1$:

$$\text{APEN}(m,r,N) = \Phi^m(r) - \Phi^{m+1}(r). \tag{10}$$

Thus APEN(m,r,N) measures the logarithmic frequency that similar runs (within the filter r) of length m also remain similar when the length of the run is increased by 1. Thus small values of APEN indicate regularity, given that i increasing run length m by 1 does not decrease the value of $\Phi^m(r)$ significantly (i.e., regularity connotes that $\Phi^m[r] \approx \Phi^{m+1}[r]$). APEN$(m,r,N)$ is expressed as a difference, but in essence it represents a ratio; note that $\Phi^m[r]$ is a logarithm of the averaged $C_i^m(r)$, and the ratio of logarithms is equivalent to their difference. A more comprehensive description of APEN may be found in Refs. [34,36].

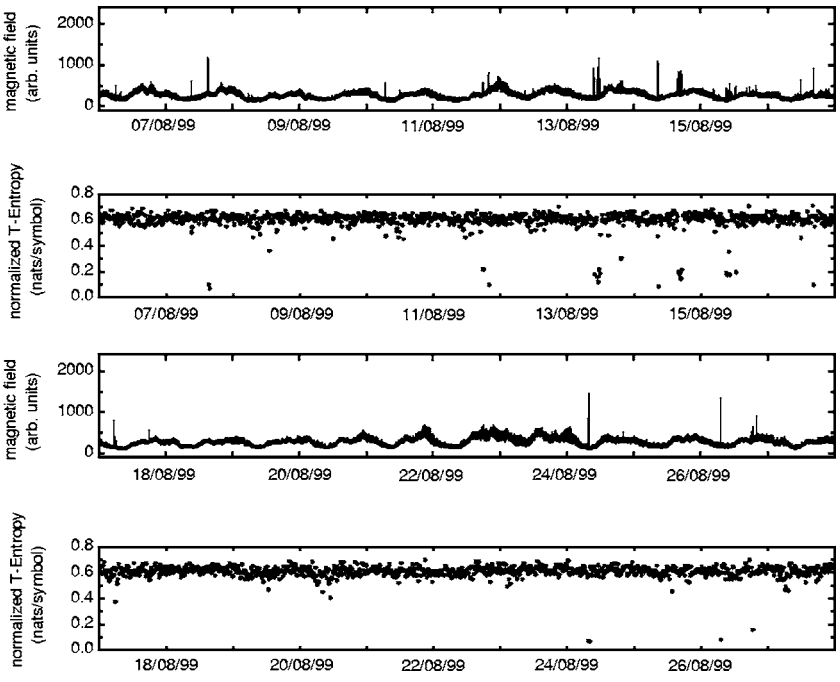

FIG. 8. The first and third panels depict the EM time series recorded by the 3-kHz (E-W) loop antenna far before the Athens EQ occurrence. Thus this EM time series describes the background of the EM recordings, i.e., the 3-kHz EM noise, in the region of the Zante station. In panels 2 and 4 each point denotes the normalized T-entropy calculated by considering consecutive time windows of 1024 elements, i.e., of duration 1024 s. The high T-entropy values indicate an underlying high complexity, as expected.

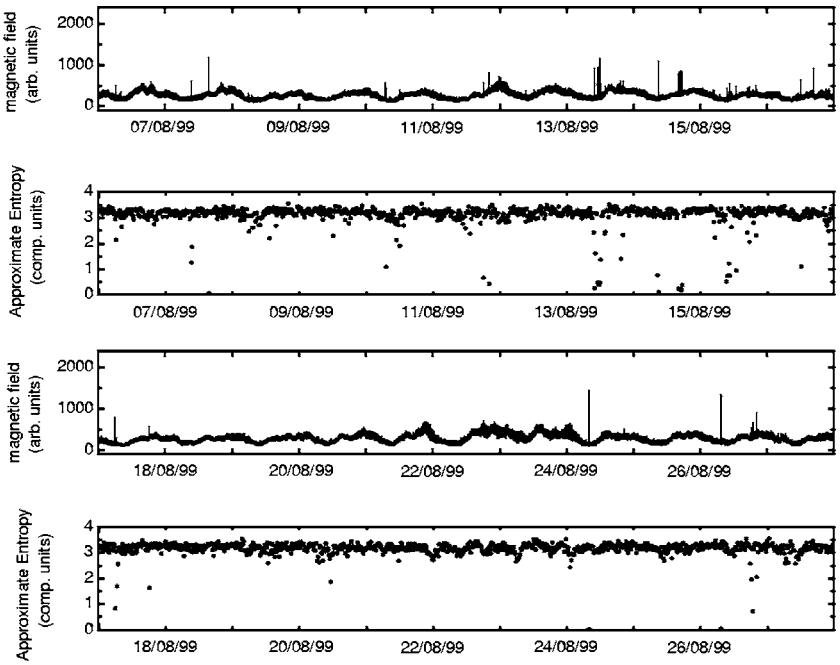

FIG. 9. Similar as in Fig. 8 but in terms of approximate entropy.

In summary, APEN is a "regularity statistics" that quantifies the unpredictability of fluctuations in a time series. Intuitively, one may reason that the presence of repetitive patterns of fluctuation in a time series renders it more predictable than a time series in which such patterns are absent. APEN reflects the likelihood that "similar" patterns of observations will not be followed by additional "similar" observations. A time series containing many repetitive patterns has a relatively small APEN; a less predictable (i.e., more complex) process has a higher APEN.

V. APPLICATION TO THE DATA

T-complexity and approximate entropy serve as measures of "complexity" of the signal: the lower the value of

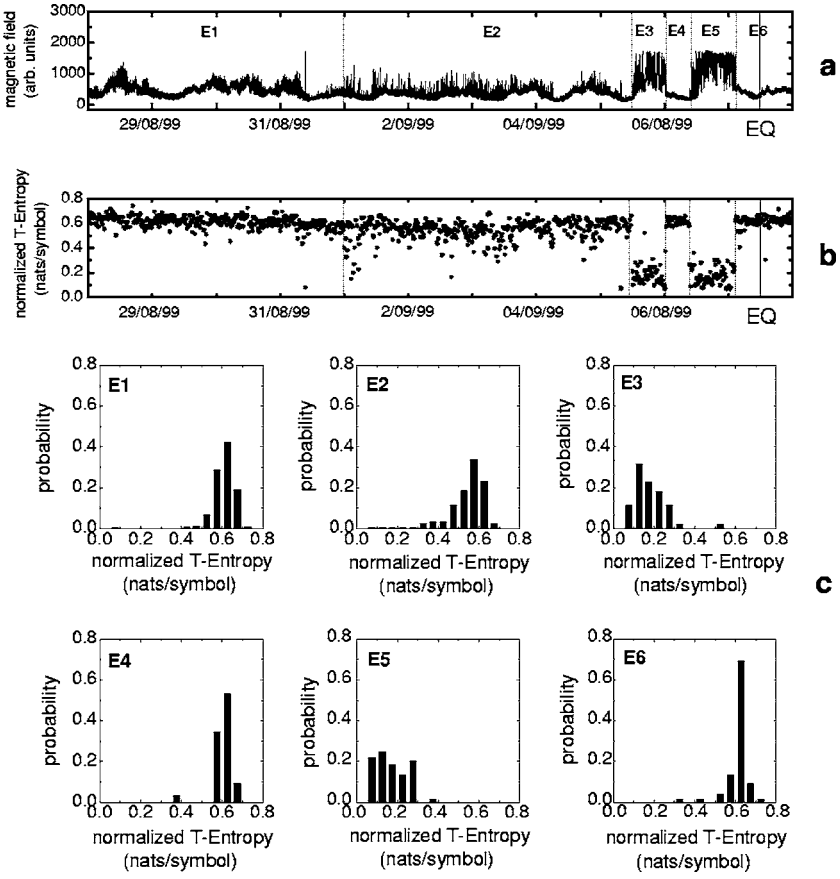

FIG. 10. (a) The EM time series recorded by the 3-kHz (E-W) loop antenna during the last days prior to the Athens EQ occurrence. (b) Each point denotes the normalized *T*-entropy calculated by considering consecutive time windows of 1024 elements, i.e., of duration 1024 s. Based on the temporal evolution of the estimated *T*-complexity values, we divide the EM time series in six distinct consecutive epochs depicted in the upper panel. (c) The distributions of the *T*-entropy values in the aforementioned six epochs offer a better quantitative description of the evolution of the *T*-complexity.

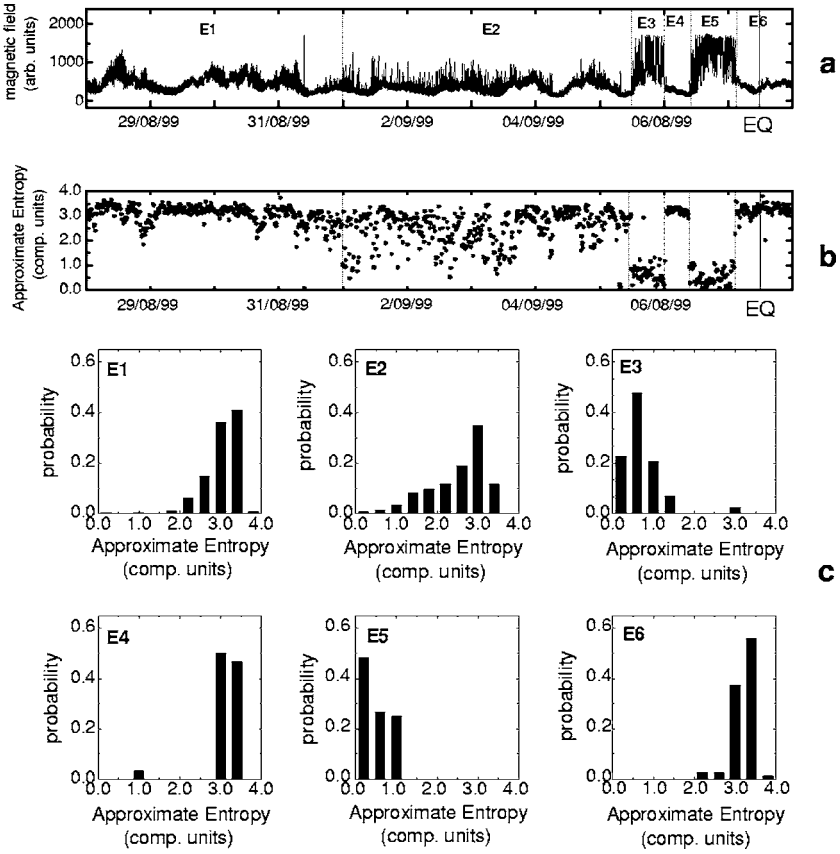

FIG. 11. Similar as in Fig. 10 but in terms of approximate entropy.

T-complexity or approximate entropy, the more "ordered" it is. We claim that our results suggest an important principle, i.e., systematic significant complexity decrease prior to an important EQ. This could be used as a diagnostic tool for Earth's crust failure.

We clarify that the real *T*-entropy corresponds to the optimal partition. The corresponding entropylike quantities for the other partitions are pseudoblock *T*-entropies. The optimal partition is this one that maximizes the *T*-entropy [33]. For this purpose, the threshold C is initially fixed to the mean value of the data in the particular time window under study. For the corresponding symbolic sequence we estimate the associated "pseudoblock *T*-entropy." We repeat the above procedure by changing the threshold c around the mean value. Our analysis indicates that the optimal partition corresponds always to a threshold not very far from the mean value of the segment. This result is depicted in Fig. 7.

We note that for every length of alphabet, there is one partition which is optimal, and which leads to the real *T*-complexity. First, we follow a standard work by Steuer *et al.* [33], and we work with binary partitions (Fig. 7). Afterwards, we extend the above considerations to more complicated cases (Fig. 12).

On the other hand, the approximate entropy was computed for a variety of r values proposed by previous researchers and it was found that the optimum value yielding clearest discrimination was the value $r=0.25$ STD, where STD is the standard deviation of the time series.

A. Case of the Athens earthquake

Following the method suggested in Sec. IV, we calculate the (normalized) *T*-entropy and APEN with the help of successive time windows, each one consisting of 1024 samples.

Figures 8 and 9 show the *T*-entropy and APEN values correspondingly far before the EQ occurrence. Hence these values characterize the background of the EM recording, i.e., the EM noise, in the region of the Zante station. The observed high *T*-entropy and APEN values indicate an underlying strong degree of complexity, as expected.

Figures 10(b) and 11(b) show the estimated *T*-entropy and APEN values correspondingly during the last days before the Athens EQ occurrence. Based on the temporal evolution of the *T*-entropy and APEN values, we can divide the signal into six consecutive different epochs (E1–E6) (see Sec. IV), depicted in Figs. 10(a) and 11(a). The distributions of the *T*-entropy and APEN values in the above six epochs, shown in Figs. 10(c) and 11(c), offer a better quantitative description of the evolution of the *T*-complexity and APEN, respectively, as the system approaches towards the catastrophic event.

Figures 10 and 11 show that the *T*-entropy and APEN values in the first, fourth, and sixth epoch have similarly high values as those of the EM noise depicted in Figs. 8 and 9. This finding suggests that the aforementioned three epochs also describe the EM background (noise) in the region of the station.

The second epoch (Figs. 10 and 11) includes a population of fractoelectromagnetic events sparsely distributed in time. These candidate precursors have lower complexity in comparison to the complexity of the EM background. The strong intermittent character of the emerged organized events may result by the fracture of the heterogeneous material in the focal area. Indeed, when a heterogeneous material is

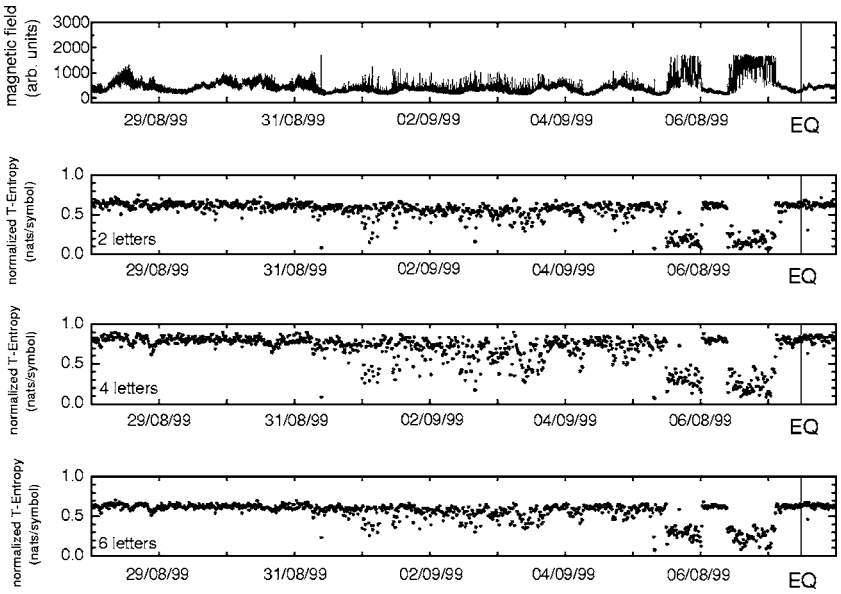

FIG. 12. The first panel depicts the EM time series recorded by the 3-kHz (E-W) loop antenna during the last days prior to the Athens EQ occurrence. The second, third, and fourth panels show the normalized T-entropy calculated by considering consecutive time windows of 1024 elements, i.e., of duration 1024 s, for alphabets of two, four, and six letters, correspondingly.

strained, its evolution toward breaking is characterized by the nucleation and coalescence of cracks before the final breakup, while the areas with a low threshold of breaking alternate with stronger volumes of the medium, where the fracture growth stops.

We now turn our attention to the third and fifth epochs. The launch of these epochs from the background is understood as an ensemble of intense fractoelectromagnetic events, which have a much lower degree of complexity even in respect to those reported in the second epoch. We emphasize that herein the vast majority of the time windows systematically exhibits a high order of organization indicating a strong influence of excitation of an event on succeeding events. These footprints may lead to the fracture of the backbone of asperities in the focal area. Indeed, for times close to breakthrough, the family of relatively homogeneous asperities of high strength sustains the elastic strain energy in the focal area. In the limit of a homogeneous system, once a crack nucleates, the stress is enhanced at its tip and therefore the next crack almost surely develops at the tip. Hence one does see a strong influence of excitation of an event on succeeding events in the associated part of the recorded time series.

Sufficient field and laboratory experimental evidence, as well as theoretical arguments, enhance the hypothesis that the two strong EM bursts, emerged in the tail of the precursory EM activity, are associated with the fracture of asperities (see Sec. VII).

Remark: We have also tried normalized T-entropy computations for alphabets of four and six letters. The results roughly remain the same concerning the discrimination of the above suggested epochs (Fig. 12).

B. Case of the Kozani-Grevena earthquake

We first refer to the case of the MHz precursory emission [Fig. 3(a)]. We divide the time series in consecutive time windows, each of 1024 elements, we calculate the T-entropy and APEN values of these segments of short duration, and then we study the temporal evolution of the estimated values (Figs. 13 and 14). We do not observe any significant alteration of complexity as the catastrophic event approaches.

Remark: Symbolic dynamics provides a rigorous way of looking at the "real" dynamics with finite precision. Based on symbolic dynamics, one loses an amount of detailed information, but some of the robust properties of the dynamics may be kept. Thus the study in terms of T-entropy is a way of coarse-graining or reduction of description. On the other hand, the approximate entropy method embeds the original

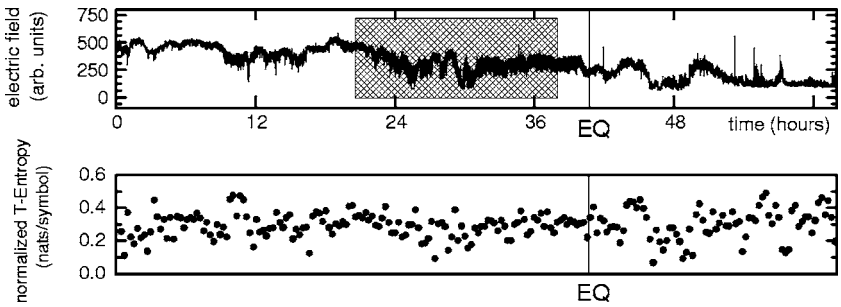

FIG. 13. The upper panel depicts the EM anomaly detected at Zante station at 41-MHz dipole $\lambda/2$ antenna preceding the Kozani-Grevena EQ. In the lower panel, each point denotes the normalized T-entropy calculated by considering consecutive time windows of 1024 elements, i.e., of duration 1024 s. We do not observe any characteristic precursory pattern in terms of T-entropy as the catastrophic event approaches. We note that on the contrary the fractal spectral analysis reveals rich information concerning the preparation of the impending EQ [19–21].

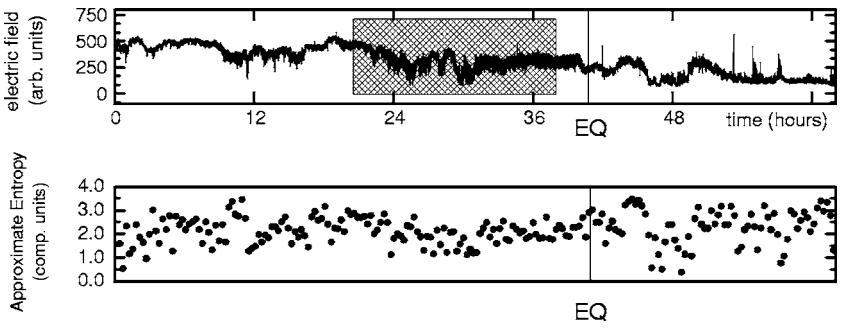

FIG. 14. Similar to Fig. 13 but in terms of approximate entropy.

time series in a two-dimensional phase space only. As a result, the two methods could not be pertinent for a detailed description of a high complexity process. Consequently, there are two possibilities: (i) there is not any precursory pattern in the recorded MHz signal; (ii) there is an underlying complex fractoelectromagnetic emission that preserves a high order of complexity; thus the applied methods are not sensitive enough to distinguish the launch of this stage from the EM background (noise). We note that the fractal spectral analysis reveals rich information hidden in this preseismic EM activity [19,20] supporting the second suggestion (see Secs. VI and VII).

Now we study the strong kHz precursory emission which appeared just before the EQ occurrence [Fig. 3(b)]. We compute the *T*-complexity and APEN values in ten distinct segments (W1–W10), as depicted in Figs. 15 and 16, respectively. The segments are chosen arbitrarily, except for the case of the window W8 which includes the strong impulsive preseismic signal. In Figs. 15 and 16 we observe a significant decrease of *T*-complexity and APEN during the emergence of the burst (W8). This behavior is contrary to that of all other windows. We can conclude that all the windows, except the window W8, refer to the EM noise, which is characterized by high complexity. On the opposite, the intense kHz emission emerging during the time window W8, namely, just before the EQ occurrence, indicates the appearance of a new strongly organized fractoelectromagnetic mechanism.

We emphasize that the low *T*-entropy and APEN values in the strong kHz EM burst abruptly appeared in the tail of the preseismic emission (Figs. 15 and 16) comparable to the low *T*-entropy and APEN values in the two strong kHz bursts abruptly emerged in the end of the EM activity associated with the Athens EQ (Figs. 10 and 11). This similarity indicates that in both cases the epoch of the sudden significant reduction of *T*-complexity and approximate entropy may reflect the final stage of the EQs generation, i.e., the fracture of asperities in the focal area (see Sec. VII).

C. Nonlinear methods: A recapitulation

The temporal evolution of both *T*-complexity and APEN implies two distinctive candidate seismogenic epochs in the case of Athens. We give emphasis to fact that the existence

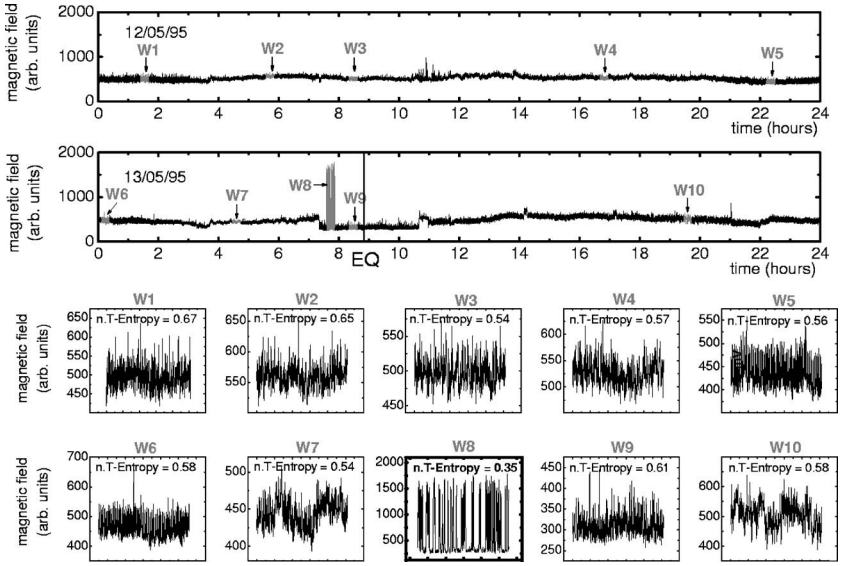

FIG. 15. The first and second panels depict the EM time series recorded by the 3-kHz (vertical) loop antenna. The solid line indicates the time of the Kozani-Grevena EQ. The grey color indicates ten distinct time windows W_i in the time series. The third and four panels show a magnification (zoom) of the signal for windows W1–W10. We record the corresponding *T*-entropy in each window. We stress the significant reduction of the *T*-entropy, during the grey window W8. This behavior could indicate that the abrupt emergence of the strong 3-kHz EM anomaly signifies the appearance of a new phase in the EQ preparation process, which is characterized by a significantly higher organization.

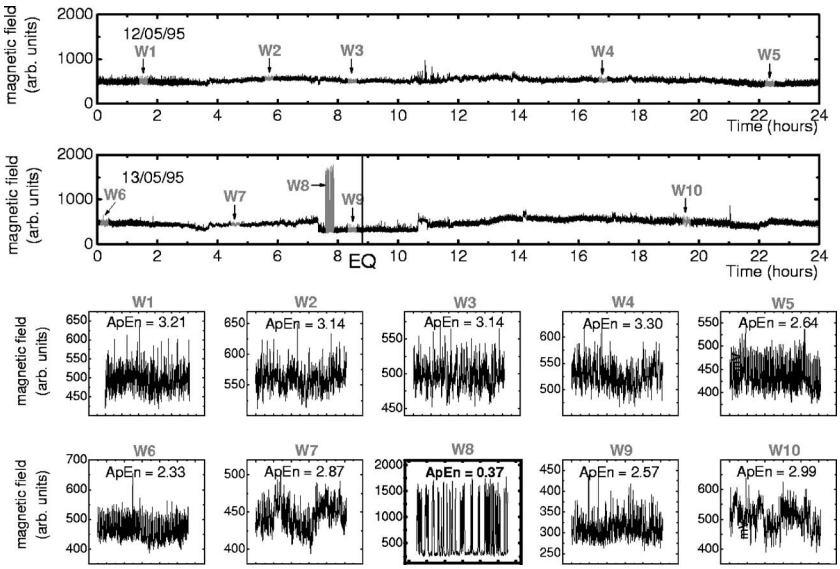

FIG. 16. Similar to Fig. 15 but in terms of approximate entropy.

of these two epochs is described in exactly the same manner by both kinds of nonlinear analysis. The first epoch includes a number of organized kHz EM events that appear in a sporadic fashion. This epoch may correspond to the fracture of the heterogeneous material in the focal area. The second epoch includes an ensemble of strong events compactly distributed in time having a significantly higher order of organization. This epoch may refer to the fracture of the backbone of asperities that sustain the system. We point out that a collection of strong kHz EM pulses, having a very low complexity, abruptly also emerged just before the Kozani-Grevena EQ occurrence.

Finally, the applied nonlinear methods do not extract any precursory signature in the MHz EM anomaly associated with the Kozani-Grevena EQ. We note that the linear fractal spectral analysis that follows reveals symptoms of the impending shock in this activity.

VI. ANALYSIS IN TERMS OF SPECTRAL FRACTAL ANALYSIS

Ample experimental and theoretical evidence indicates that as the final failure in the disordered media is approached the underlying complexity manifests itself in linkages between space and time, generally producing patterns on many scales and the emergence of fractal structure close to nonequilibrium phase transitions. Thus a lot of work on complexity focuses on statistical power laws that describe the scaling properties of fractal processes and structures. Based on these concepts, we focus on the statistics of the fluctuations in the preseismic time series with respect to their amplitude, say $A(t_i)$. If the time series $A(t_i)$ is a temporal fractal, that series cannot have a characteristic frequency. The only possibility is then that the power spectrum $S(f)$ has a scaling form

$$S(f) \sim f^{-\beta}, \tag{11}$$

where f is the frequency of the Fourier transform (FT). In a $\log S(f) - \log f$ representation the power spectrum is a line with spectral slope β. The linear correlation coefficient r is a measure of the goodness of fit to the power law (11).

The "global wavelet spectrum" is used in order to provide an unbiased and consistent estimation of the true power spectrum of the time series. The continuous wavelet transform based on the Morlet wavelet makes the calculation.

We calculate the parameters β, r dividing the signal into successive segments of 1024 samples each. Thus we have the possibility *to study not only the presence of a power law but also the evolution in time of the associated parameters* β, r.

A. Application to the case of the Athens earthquake

Two classes of signal have been widely used to model stochastic fractal time series [37,38]: fractional Gaussian noise (FGN) and fractional Brownian motion (FBM). These are, respectively, generalizations of white Gaussian noise and Brownian motion. For the case of the FBM model the scaling exponent β lies between 1 and 3. On the contrary, the regime of FGN is indicated by β values from -1 to 1.

Figure 17 shows the evolution of β, r values far from the catastrophic event. We observe that a population of time windows behaves as a fractional Gaussian noise, while a number of them do not have any fractal properties.

Figure 18 shows the estimated β, r values during the last days prior to the Athens EQ. Based on the temporal evolution of this parameter, we can divide the signal into six consecutive different epochs (E1–E6) depicted in this figure. Figure 19 depicts the histograms of probability distribution of the β, r values calculated on 1024 measurement segments for the six epochs defined in Fig. 18.

The β, r values in the first, fourth, and sixth epoch have similar values as those depicted in Fig. 17. This finding suggests that the aforementioned three epochs also describe the EM noise in the region of the station.

We focus on the second, third and fifth epoch. The second epoch includes a population of fractoelectromagnetic events that show a fractional Brownian motion (FBM) behavior. The observed transition from the FGN to FBM behavior reflects the appearance of organization in the underlying frac-

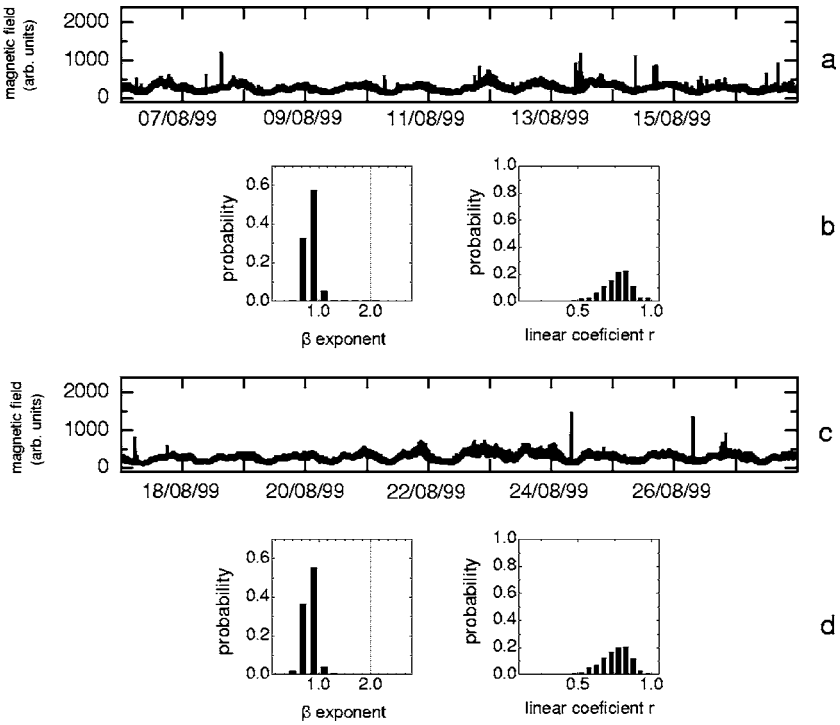

FIG. 17. Panels (a) and (c) show the EM time series recorded by the 3-kHz (E-W) loop antenna far before the time of Athens EQ occurrence. Panels (b) and (d) depict the histograms of probability distribution of the correlation coefficient r and exponent β calculated on 1024 measurements segments for the time series including in the panels (a) and (c) correspondingly. We observe that the time series under study, which describes the EM noise in the region of the station, either follows the fractional Gaussian noise model or does not have any fractal property.

toelectromagnetic mechanism. Figure 19 also reveals a significant increase of r values within the two strong bursts, namely, within the E3 and E5 epochs. Indeed, therein, the fit to the power law (11) is excellent: a region with r close to 1 is approached. This implies that the preseismic activity within these two windows could be ascribed to a multi-time-scale cooperative activity of numerous activated cracks. An individual unit's activity is dominated by its neighbors, so that all units simultaneously alter their behavior to a common compact fractal structure. Figures 18 and 19 also show an important shift of β exponents towards higher values during the emergence of the two impulsive signals. The estimated β values $(2<\beta<3)$ within E3 and E5 epochs corroborate the presence of strong memory in the underlying fractoelectromagnetic process: the EM fluctuations show strong correlations, namely, the system refers to its history in order to define its future. The increase of β values means that the spectrum manifests more power at lower frequencies than at

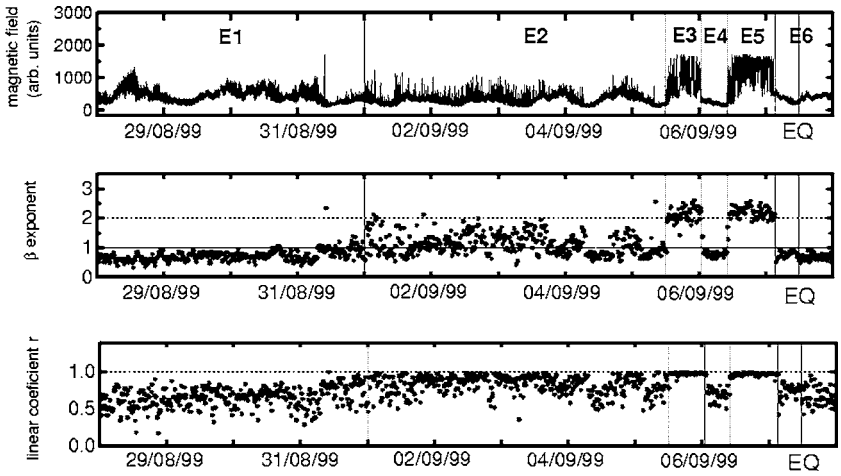

FIG. 18. The upper panel shows the EM time series recorded by the 3-kHz (E-W) loop antenna during the last days before the Athens EQ. The medium and lower panels describe the temporal evolution of the β exponent and linear coefficient r, respectively, calculated on consecutive segments of 1024 measurements each. Based on the temporal evolution of the estimated β values and r values we divide the EM time series in six distinct consecutive epochs E1–E6 depicted in the upper panel. We observe that the first, fourth, and sixth epochs follow the fractional Gaussian model $(\beta<1)$, as the epoch far before the EQ (Fig. 17), indicating that these three epochs correspond to the EM background (noise) in the region of the station. Epoch E2 follows the fractional Brownian motion model having antipersistent properties $(1<\beta<2)$, and finally, epochs E3 and E5 follow the fractional Brownian motion model having persistent properties $(2<\beta<3)$. We emphasize that the aforementioned six distinct epochs are identical with the six distinct epochs defined by the temporal evolution of both T-entropy and approximate entropy (see Figs. 10 and 11).

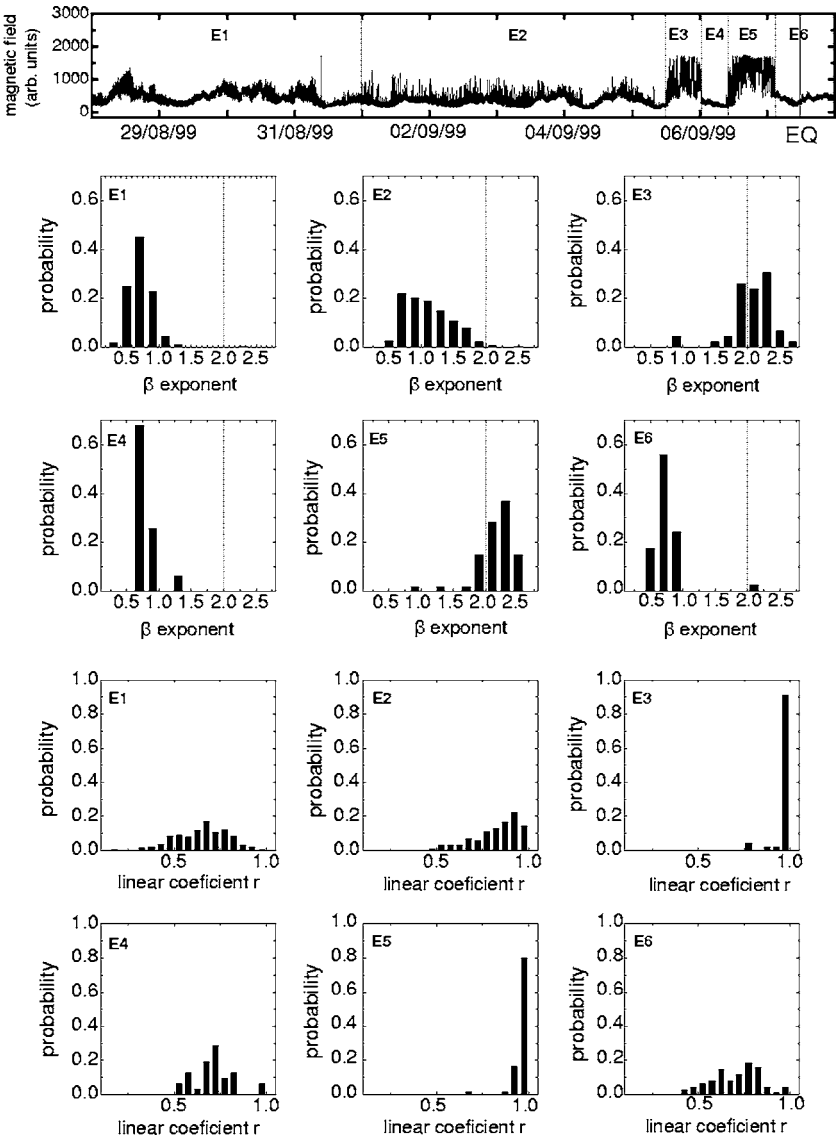

FIG. 19. Histograms of probability distribution of the correlation coefficient r and exponent β calculated on 1024 measurement segments for the six epochs defined in Fig. 18. This description offers a better quantitative explanation of the evolution of these parameters, as the system approaches the catastrophic event. We emphasize that the temporal evolution of the r exponent also divides the time series in six distinct epochs. We pay attention to the fact that the fit to the power law $S(f) \sim f^{-\beta}$ is continuously excellent during epochs E3 and E5.

high frequencies, i.e., indicates the enhancement of lower frequency fluctuations. This behavior may indicate that the opening cracks interact and coalesce to form larger fractal structure during the epochs E3 and E5. The reported at the same time accelerating energy release further indicates that during these two time intervals the prefocal area is not only near to the "critical point" in the sense of having power-law correlations, but also in terms of exhibiting high susceptibility to perturbations. Indeed, due to the high level of the clustering of opening cracks, even a new small cluster, if it connects large clusters, may generate a significant event.

B. Transition from the antipersistent to the persistent regime

The β exponent is related to the Hurst exponent H by the formula

$$\beta = 2H + 1 \quad \text{with } 0 < H < 1 \tag{12}$$

for the FBM model [37,38].

The exponent H characterizes the persistent or antipersistent properties of the signal [3]. The range $0 < H < 0.5$, $(1 < \beta < 2)$ indicates an antipersistency, reflecting that increases in the value of a time series are likely to be followed by decreases and conversely. Physically, this implies a set of fluctuations tending to induce a stability to the system, namely a nonlinear feedback system that "kicks" the opening rate away from extremes. The range $0.5 < H < 1$, $(2 < \beta < 3)$ indicate persistent behavior. The signal shows persistent properties during the emergence of the two strong EM bursts (see Figs. 18 and 19). This means that increases in the value of a time series are likely to be followed by increase, namely the system has been starting to self-organize by a positive feedback process. Thus the launch of the persistent activity could give a significant hint of a considerable probability for a forthcoming significant seismic event. It is worth mentioning that laboratory experiments by means of acoustic and EM emission also show that the main rupture occurs after the appearance of persistent behavior [39–42].

C. Application to the case of the Kozani-Grevena earthquake

The fractal spectral analysis of the MHz and kHz EM activities recorded prior to the KG EQ reveals rich informa-

tion indicating the approach to the global instability [19–21]. Based on the behavior of the Hurst exponent we also distinguish two different regimes in the whole preseismic EM activity. Indeed, the initial MHz activity [Fig. 3(a)] is characterized by antipersistent properties and it could be originated during the fracture of heterogeneous medium that surrounds the family of asperities in the focal area [19–21]. Moreover, we have shown that the evolution of the time series during the shaded time interval in Figs. 13 and 14 is expected in the framework of the hypothesis that the fracture in the highly disordered media develops as a kind of generalized continuous phase transition (see Fig. 2 in Ref. [19]): considerations of symmetry breaking indicate that the system is gradually driven out of equilibrium. On the contrary, the kHz EM activity, which abruptly emerged just before the EQ occurrence [Fig. 3(b)], shows strong persistent behavior [19–21]. The appearance of persistent properties may indicate that the process is being driven as nonequilibrium instability [19–21], as well as this radiation could be radiated during the fractures of backbone of asperities in the focal area.

D. Spectral fractal analysis: A summary

Based on the temporal evolution of the estimated Hurst exponents we distinguish two different epochs in the evolution of the precursory EM activity. Both epochs follows the fractional Brownian motion model and emerged from the background that follows the fractional Gaussian noise model. However, the first epoch shows antipersistent properties, while the second one is characterized by persistent behavior.

VII. SYNOPSIS AND DISCUSSION

In this paper, we study, in terms of nonlinear and linear techniques, whether precursory features emerged in preseismic EM time series indicating the approach of global failure. More precisely, in order to examine transient phenomena we divide the measurements into time windows of small duration and analyze them. If this analysis yields different results for some precursory epochs, then corresponding transient stages of the EQ preparation process can be extracted. The analysis suggests that the preseismic EM signals provide a way of observing the Earth's crust ability to respond to stresses: the Athens and Kozani-Grevena EQs seem to register on the EM sensors of the Zante station.

First, based on the temporal evolution of T-complexity and approximate entropy we distinguish two candidate seismogenic epochs that emerged from the background. The first one includes a number of EM events that show lower complexity in comparison to the background. The emerged organized EM events are sparsely distributed in time during this epoch. The second candidate seismogenic epoch is characterized by the launch of a population of strong EM events having much lower complexity in respect to those of the first epoch; these characteristic events are densely distributed in time during this epoch. In the following, based on the temporal evolution of Hurst exponent, we also distinguish two candidate seismogenic epochs. Both epochs follow the fractional Brownian motion model and emerge from the background that follows the fractional Gaussian model. However, the first epoch is characterized by antipersistent properties, and the second one by persistent behavior. We underline the fact that the first and second epochs, obtained by the nonlinear methods, coincide with the two epochs, obtained by the independent linear fractal spectral analysis: the first epoch of higher complexity corresponds to the antipersistent epoch and the second epoch of much lower complexity corresponds to the persistent epoch.

The features that distinguish the aforementioned two candidate seismogenic epochs suggest that the first epoch may correspond to the stage of the fracture of the heterogeneous medium that surrounds the backbone of asperities, while the second epoch may describe the stage of fracture of the family of asperities. Hence a central thesis of the present work is taken together: the significant systematic reduction of both T-entropy and approximate entropy, in combination with the emergence of strong persistent behavior, may reveal the fracture of backbone of the asperities in the focal area.

It would be desirable to have the possibility to analyze more preseismic EM emissions. However, the collection of a volume of appropriate EM data for statistical purposes requires some decades of years at least. Surface EQs with magnitude 6 or larger, which happen in continental Greece, occur in a very slow rate, so that a statistical evaluation stemming from the EM data is practically impossible. On the other hand, it is in principle difficult to prove association between any two events (possible precursors and EQs) separated in time. This obliges us to attempt a multidisciplinary evaluation adjusted to the candidate seismogenic footprints, based on available theoretical arguments, relevant laboratory measurements, and associated independent field information.

A. Theoretical arguments

1. In analogy to the study of critical phase transitions in statistical physics, it has been recently proposed that the fracture of heterogeneous materials could be viewed as a critical phenomenon [43] either at laboratory scale [44] or at geophysical scale [45]. Based on a recently presented statistical method of analysis for the critical fluctuations in systems which undergo a continuous phase transition at equilibrium (Ref. [21], and references therein), we have suggested [19] that the initial antipersistent part of the precursory EM activity finds his origin in the fracture of the heterogeneous material in the focal area and could be described in analogy with a thermal continuous phase transition. On the contrary, the abruptly emerged final persistent part is thought to be due to the fracture of asperities that sustain the system. The evolution of the persistent phase implies a nonequilibrium process.

2. We have paid attention to the transition from antipersistent to persistent behavior. A basic reason for our interest in complexity is the striking similarity in behavior close to irreversible phase transitions among systems that are otherwise quite different in nature [46]. Interestingly, theoretical studies suggest that the final EQ and neural-seizure dynamics should have many similar features and could be analyzed within similar mathematical frameworks [47]. Recently [22],

by monitoring the temporal evolution of the fractal spectral characteristics in EEG (electroencephalograph) recordings on rat experiments and preseismic electromagnetic (EM) time series associated with Athens EQ, we showed that many similar distinctive symptoms (including common alterations in associated scaling parameters) emerge as epileptic seizures and EQs are approaching. We emphasize that both catastrophic events happen after the occurrence of persistent behavior. In both cases the transition from antipersistent to persistent behavior indicates that the onset of a severe crisis is imminent.

3. Recently, the research area known as "fractal electrodynamics" has been established. This term was first suggested by Jaggard [48] to identify the newly emerging branch of research, which combines fractal geometry with Maxwell's theory of electrodynamics. From the laboratory scale to the geophysical scale, fault displacements, fault and fracture trace length, and fracture apertures follow a power-law distribution, e.g., as

$$N(>l) \sim l^{-\zeta}, \tag{13}$$

where $N(l)$ denotes the cumulative number of fractures larger than l, and ζ is the fractal dimension (Ref. [18] and references therein). Thus a fault shows a fractal pattern: a network of line elements having a fractal distribution in space is formed as the event approaches. However, as it said, an active crack or rupture can be simulated as a radiating element. The idea is that a "fractal electromagnetic geo-antenna" can be formed as an array of line elements having a fractal distribution on the ground surface as the main event is approached. We have tested this idea in terms of fractal electrodynamics. We have shown that the evolution of the preseismic kHz-MHz emissions associated with the KG and Athens EQs are governed by characteristics (e.g., scaling laws, temporal evolution of the spectrum content, broad band spectrum region, and accelerating emission rate) predicted by fractal electrodynamics [18]. The fractal tortuous structure can significantly increase the radiated power density, as compared to a single dipole antenna. The tortuous path increases the effective dipole moment, since the path length along the emission is now longer than the Euclidean distance [18], and thus the possibility to capture these preseismic radiations by aerial antennas.

B. Laboratory measurements

Although there remain significant problems in extrapolating laboratory results to field conditions, sufficient experimental evidence supports the suggestion that the emergence of strong positive correlations in the kHz EM activity reflects the faulting nucleation phase. We mention here some relevant observations.

1. Experiments in terms of acoustic emission reveal a significant shift from MHz to kHz just before global failure (97–100 % of the failure strength) (Ref. [17] and references therein). As mentioned earlier the strong persistent kHz emission emerges at the tail of the EM activity associated with the Athens and Kozani-Grevena EQs.

2. Recent experiments in terms of both acoustic and EM emission show that the main rupture occurs after the appearance of strong persistent behavior in the corresponding prefracture time series [39–42].

3. Laboratory studies under well-controlled conditions, i.e., using well-prepared samples containing well-known asperities, should be useful for understanding the physics of asperities. Recently Lei and co-workers, [42,49] have studied how an individual asperity fractures, how coupled asperities fracture, and also the role of asperities in fault nucleation and as potential precursors prior to dynamic rupture. These observations reveal a strong similarity between the fracture of asperities in laboratory scale experiments and tectonic-scale events. More precisely, the authors suggest the following:

a. Intense microcracking may occur in a strong asperity when the local stress exceeds the fracture stress of the asperity. This feature is in agreement with our results.

b. The self-excitation strength, which expresses the influence of excitation of an event on succeeding events or, equivalently, the degree of positive feedback in the dynamics, reaches a maximum of ~ 1 during the nucleation phase of the fault. Recall that the Hurst exponent also approaches its maximum value of 1 in the tail of the precursory EM radiation.

c. The fractal dimension decreases from ~ 2.2 in the pre-nucleation phase to 1.0–1.4 during asperity fracture. The authors correlate the decrease of the fractal dimension with the concentration of stresses around the family of asperities. The fractal dimension d of the EM time series is found from the relation $d=2-H$ for the FBM class. After considering the observed H values (see Sec. VI) we conclude that the detected kHZ EM time series prior to the Athens EQ exhibits a fractal dimension from 1.2 to 1 in its tail, i.e., within the precursory two strong EM bursts. This evidence implies the concentration of stresses around the family of asperities. We recall that a few days prior to the Athens event, the seismicity was centered at the epicenter area, i.e., at a distance of about one source dimension (<30 km) from the Athens EQ epicenter (Ref. [23] and references therein).

4. The statistical analysis of the EM anomalies detected prior to the Athens EQ suggests that both the amplitudes and energies of the "EM events" follow power-law distributions with exponents consistent with other critical realizations obtained there via real laboratory measurements, theoretical predictions, or computer simulations even with earthquakes. Characteristically, the cumulative number $N(>A)$ of preseismic EM pulses having amplitude larger than A follows the power law $N(>A) \sim A^{-b}$ [3]. On the other hand, Rabinovitch *et al.* [9] have studied the fractal nature of EM radiation induced in rock fracture. The analysis of the prefracture EM time series reveals that the cumulative distribution of the amplitudes in the laboratory also follows a power law with exponent 0.62. The observed scaling similarity of EM emissions during multiple fractures in solid materials from the laboratory scale up to the geophysical scale strongly support the hypothesis that the detected emissions in the field have been generated during crack opening in the focal area.

5. Laboratory studies and theoretical arguments suggest that the damage localization and sensitivity of energy release characterize the fracture surface formation, and thus provide two cross-checking precursors for the prediction of rupture [50]. Indeed, a few days prior to the Athens event, the seis-

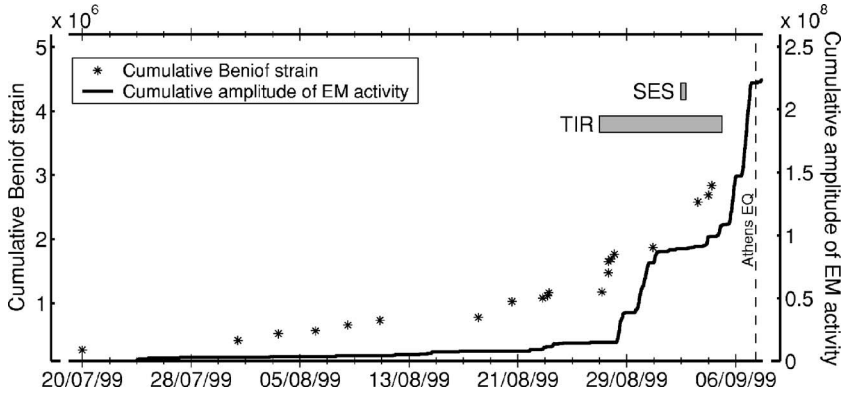

FIG. 20. The following precursors have been reported in the indicated time intervals during the last days before the Athens EQ: (i) An accelerating seismic energy release in the critical area around the epicenter of the Athens event: the sequence of stars (*) denotes the evolution of the Benioff cumulative strain (seismic energy) energy as the event is approaching. (ii) An accelerating kHz EM emission: the solid line describes the evolution of the Benioff-type cumulative kHz EM energy release. We draw attention to the similarity of the temporal evolution of both the mechanical and the EM energy release. (iii) A sequence of thermal infrared radiations that exhibits a progressive increase of its intensity in the area around the focal zone. (iv) An independent SES activity (ultralow-frequency geoelectric potential differences). Moreover, SAR interferometry (see text) leads to a fault modeling of the Athens EQ that strongly coincides in the energy domain with the detected precursory kHz EM emission. Maybe the Athens EQ is a unique case where a set of different precursory phenomena has been recorded during the last days before the shock, giving converging estimations. The aforementioned experimental information enhances the hypothesis that the Athens EQ registers on the kHz EM sensors.

micity was centered at a distance of about one source dimension (<30 km) from the Athens EQ epicenter [23] and simultaneously the rate of both the seismic and EM energy release exhibited a significant power-law type increase (Fig. 20).

6. Numerical and laboratory [51] results predict an abrupt initiation of the nucleation phase. An inspection in Figs. 2 and 3(b) verifies that the kHz strong multipeaked signals on the tail of the precursory kHz emissions emerged with sharp onsets.

C. Field information

Ample field information strongly supports the association of the recorded EM anomalies with the fracture of asperities. First we focus on the Athens EQ.

1. Synthetic aperture radars (SAR) are space-borne instruments that emit EM radiation and then record the strength and time delay of the returning signal to produce images of the ground. By combining two or more SAR images of the same area, it is possible to generate elevation maps and surface change maps with unprecedented precision and resolution. This technique is called SAR interferometry. SAR interferometry is becoming a new tool for active tectonics by providing both mm-precision surface change maps spanning periods of days to years and m-precision, high-resolution topographic maps for measuring crustal strain accumulated over longer periods of time. The fault modeling of the Athens EQ, based on information obtained by radar interferometry (ERS-2 satellite) [52], predicts two faults: the main fault segment is responsible for 80% of the total energy released, with the secondary fault segment for the remaining 20%. A recent seismic data analysis carried out by Kikuchi, using the now standard methodology, also indicates that a two-event solution for the Athens EQ is more likely than a single event solution [16,23]. According to Kikuchi, there was probably a subsequent (M_w=5.5) EQ after about 3.5 s of the main event (M_w=5.8). On the other hand, the first strong EM burst at the tail of the associated kHz preseismic EM emission (Fig. 2) contains approximately 20% of the total EM energy received during the emergence of the two bursts, and the second the remaining 80% [16]. This surprising correlation in the energy domain between the two strong preseismic kHz EM signals and two faults activated in the case of the Athens EQ, strongly supports the hypothesis that the two strong EM bursts reveal the nucleation of the impending EQ.

2. Recently, statistical physicists have shown the existence of a power-law acceleration of acoustic emissions announcing the global rupture, similar to the critical behavior of the out-of-equilibrium phase transition, offering a way to predict material rupture [43]. However, it has been pointed out [45] that a power-law increase in the cummulative seismic strain release can also be expected if the rupture process is analogous to a critical phase transition. Following Ref. [45] in Fig. 20 we depict the "cumulative Benioff strain release,"

$$\epsilon(t) = \sum_i \sqrt{E_i}(t) = A - B \cdot (t_f - t)^m \tag{14}$$

computed over critical circle [45,53] R=110 km at the epicenter of the Athens EQ as a function of time, where t_f is the failure time, E_i is the mechanical energy released by the ith foreshock, and A, B, m are positive quantities [45]. In Fig. 20 we also show the "Benioff" cumulative EM energy release $\Sigma A_i(t)$ (in arbitrary units) as a function of time, where A_i is the amplitude of the ith preseismic EM pulse. We draw attention to the similarity of the temporal evolution of both the mechanical and the EM energy release as the main event approaches. This evidence further supports the hypothesis

that the detected EM precursor is a subproduct of the Athens fault system generation.

3. Infrared remote sensing makes use of infrared sensors to detect infrared radiation emitted from the Earth's surface. Enhanced thermal infrared (TIR) emissions from the area of EQ preparation a few days before the seismic shock retrieved by satellites has been frequently reported [23,54]. A clear increase in the TIR emission over the area around the Athen's EQ epicenter was detected from satellites during the days where the strong EM radiation of low complexity and persistent behavior emerged [55]. Recently, an explanation for "thermal anomalies" from a solid-state physics viewpoint has been proposed [56], namely that the IR emission is due to the radiative decay of vibrationally highly excited *O-O* bonds, which form at the rock surface during recombination of positive holes, activated by the build-up of stress in the Earth's crust. The appearance of TIR emissions further enhances the consideration that the fracture process has been extended up to the surface layers of the crust.

4. A second type of precursory signals is the so-called seismic electric signals (SES) [57]. They are ultralow-frequency (<1 Hz) changes of the electric field of the earth and are consistent with the "pressure stimulated currents model" [58], which suggests that, upon a gradual variation of the pressure (stress) on a solid, transient electric signals are emitted, from the (re)orientation of electric dipoles (formed due to disorder in the focal area), when approaching a critical pressure. Field and laboratory experience coincide to the point that the transient low-frequency electric signals (SES) tend to appear earlier. This scheme, namely, the appearance of ultralow frequency (<1 Hz) changes of the electric field of the earth following by kHz-MHz EM precursory radiations, has been reported before the Athens EQs. On 1 and 2 September 1999, a clear SES activity has been recorded in Lamia station with duration of ~ 9 h [59]. We recall that the two strong impulsive kHz EM signals have been detected during the last few decades of hours before the main event, while, the last EM burst ceased ~ 9 h before the EQ. We pay attention to the following peculiarity of the recorded SES activity: its last portion has a larger amplitude and also changes polarity. The detected precursory anomaly could be interpreted as coming from two different sources [59]. It might be argued that the information for the impending two faults activation had imprint not only in the precursory kHz EM emission [16] but also in the detected very low-frequency SES activity.

In summary, a set of different physical peculiarities has emerged prior to the Athens EQ, as follows: (i) An accelerating seismic energy release. Prior to the Athens EQ, regional seismic energy release has exhibited a power-law increase with a singularity in the time of seismic shock occurrence. (ii) An accelerating kHz EM radiation detected at the Zante station. We draw attention to the similarity of the temporal evolution of both the mechanical and the EM energy release as the main event approaches. (iii) A SES ultralow-frequency (<1 Hz) activity recorded at the Lamia station. (iv) A clear increase in the TIR emission over the area around the epicentre of the Athens EQ. Figure 20 describes the temporal evolution of these precursors. Moreover, a radar interferometry analysis leads to the fault modeling of the Athens EQ consistent with the structure of EM activity [16,52]. All these various ground and satellite observations lead to converging results. This evidence suggests that it is useful to combine various field measurements to enhance the understanding behind the generation of EQs.

Now we turn on the Kozani-Grevena case: The Kozani-Grevena EQ was preceded within 30 min of the main shock by five foreshocks with $M>3.5$ clustered within 2 km of one another about 5–10 km from the main shock epicenter [17]. Thus the unusual foreshock activity for the aseismic Kozani-Grevena region was reported a few minutes after the detection of the kHz EM anomaly and a few minutes before the EQ. Note that the size of foreshock clustering correctly fits the correlation law with the main-shock magnitude obtained for Californian EQs [60]. Hence the observed foreshocks may be possibly regarded as a fingerprint of a local dynamic rupture of asperities in the zone associated with the nucleation on the main rupture. Consequently, the idea that the preseismic persistent EM activities under study could imply an underlying structural instability that belongs to the final stage of the EQ generation could be accepted. We note that SES activities also have been detected prior to the KG EQ, i.e., on April 18, 1995 and April 19, 1995 [57].

D. Earlier field experience

In this field of research, first of all, we require that the results can be reproduced. The observations should be verified by independent experiments taking into account differences of the EQ process, regime, and so on. The Chinese experience [61] concerning the behavior of preseismic EM anomalies can be summarized in the following five points: (i) The frequency band of the detected EM anomalies is quite wide. (ii) Anomalies are detected earlier in the electric field (MHz) than in the magnetic (kHz) field. (iii) The electric anomalies last longer than the magnetic anomalies. (iv) The anomalies stop before the EQ occurs. (v) No signals are recorded while the EQ is in progress. Figures 3(a) and 3(b) show that the EM anomalies recorded before the Kozani-Grevena EQ have all these five characteristics. In the case of the Athens EQ these empirical criteria are not violated.

VIII. CONCLUSIONS

The results of the present work establish an interesting link between dynamics and information. They show that preseismic EM fluctuations are the natural carriers of information of the impending EQ preparation process. More precisely, we have seen that a combination of nonlinear with linear statistical approaches allows one to extract rich information hidden in preseismic kHz-MHz EM time series.

First, the temporal evolutions of both T-entropy and approximate entropy have been shown to bear the occurrence of two distinct precursory epochs. The first epoch is defined by the launch of EM events that have lower, in respect to the background, complexity. These organized events are sparsely distributed in time. Based on the linear spectral fractal analysis, we conclude that during this epoch the time series follows the fractional Brownian motion model having antiper-

sistent properties. The second epoch is detectable by the recording of a population of strong EM events, densely distributed in time, having significantly lower complexity in respect to the first epoch. The time series follows the fractional Brownian motion model during the second epoch, however, this time is characterized by persistent properties.

The very thesis underlying the present paper, supported by related laboratory, field, and theoretical arguments, is that the two distinct epochs could reflect the two last stages of the EQ generation process. The first epoch could be generated by the fracture of disordered material in the focal area that surrounds the family of asperities. The second one is associated with the fracture of asperities that sustain the system.

We emphasize the fact that the Athens EQ also has been registered on independent satellite instruments (synthetic aperture radars and infrared sensors), and terrestrial instruments (seismographs and electric dipoles detecting ultralow frequency seismic electric signals). The careful study of these recordings from different teams strongly supports the above thesis. The convergence of estimations from such different precursors certainly improves the understanding of the EQ creation, and thus the chance for an EQ prediction. The Athens EQ is a unique case. In this direction enhances the necessity for a many-sided experimental and theoretical examination of this catastrophic phenomenon that is still lacking for the moment.

The statistical approach to preseismic EM emissions is still in its early life. Much remains to be done to tackle systematically precursors and to develop efficient schemes. The analogy between the prefailure symptoms in the laboratory scale and the precursory footprints in the geophysical scale presented in Sec. VII needs to be justified on a more firm basis, in particular with numerical modeling.

It would be highly desirable to have the possibility to analyze more preseismic EM emissions associated with strong surface EQs that occur on land. However, such seismic events are not so common in Greece. The potential extension of this research in regions where strong surface EQs occur on land will offer the possibility for a statistical evaluation of our suggestions in the future.

To summarize the offered considerations, we point out that the present state of research in this field requires a refined definition of a possible preseismic anomaly, and also the development of more objective methods of distinguishing seismogenic emissions from nonseismic EM events.

We emphasize that we have stated very clearly in this paper our view that the occurrence of a sequence of MHz-kHz EM anomaly in the output of the detectors does not qualify by itself as a precursory signal of an important EQ.

In our analysis of the data, we first exclude the possibility that the detected signal is a result of man-made noise, geomagnetic activity, or meteorological activity. If these requirements are satisfied, we proceed to the further analysis of the sequence of the detected signals.

Laboratory experiments of fracture as well as earlier field experience indicate that global fracture and EQ precursors do include a candidate seismogenic sequence of MHz-KHz EM activity.

Taken together, the predicted prefracture EM footprints by (i) laboratory experiments, (ii) theoretical studies in terms of criticality and complexity, (iii) the new field of fractal electrodynamics, which indicates a distinct pattern that should follow a fractoelectromagnetic emission that originates during the formation of a fault having fractal structure, and (iv) earlier field experience, constitute a rather austere set of criteria which should be met by a candidate seismogenic EM activity.

Inspired by methods of nonlinear dynamics as well as on linear fractal spectral analyses, we have shown that the sequences of MHz-kHz EM activities detected prior to the Athens and Kozani-Grevena EQs follow a temporal evolution in harmony with that predicted by the aforementioned criteria.

Multidisciplinary satellite and terrestrial measurements confirm the information obtained from the MHz-kHz EM precursors associated with the Athens EQ. This enhances the validity of the criteria used for evaluating an emerged EM activity as a preseismic one. Notice that these measurements could indicate the possible position of the epicenter of the impending EQ. Although there is no general agreement to a technique which could determine the magnitude of the EQ, the appearance of such a clear sequence of different precursors seems to be associated with surface EQs that occur in land with a magnitude about 6 or larger.

It is in this way that we argue that the detected anomalies prior to the Athens and Kozani-Grevena EQs are seismogenic ones. In the present work a strict documentation has been presented for preseismic signals in the kHz and MHz frequency bands. It is very difficult for a nonfractoectromagnetic emission to follow the strict set of criteria associated with the fracture process. Thus the detected EM anomalies before the Athens and Kozani-Grevena EQs should be reliable precursors and the research method revealed in this study can enhance the reliability of EM precursors.

In any case, the complexity of EQ preparation process is enormous, and thus a huge amount of research is needed before we begin to understand it.

ACKNOWLEDGMENTS

The authors are indebted to Professor M. Titchener for useful exchange of ideas and software. We would also like to thank to Professor J. S. Nicolis, Dr. Y. F. Contoyiannis, Professor G. Nicolis, and Professor I. Kotsireas for useful discussions and support. This work has been supported by the program EPEAEK/PYTHAGORAS 70/3/7357.

[1] W. A. Curtin, Phys. Rev. Lett. **80**, 1445 (1998).

[2] J. P. Sethna, K. Dahmen, and C. R. Myers, Nature (London) **410**, 242 (2001).

[3] P. Kapiris *et al.*, Nonlinear Processes Geophys. **10**, 511 (2003); P. Kapiris, G. Balasis, J. Kopanas, G. Antonopoulos, A. Peratzakis, and K. Eftaxias, *ibid.* **11**, 137 (2004).

[4] E. Sharon, S. P. Gross, and J. Fineberg, Phys. Rev. Lett. **74**, 5096 (1995); E. Sharon and J. Fineberg, Nature (London) **397**, 333 (1999); Phys. Rev. B **54**, 7128 (1996).

[5] S. C. Langford, D. L. Doering, and J. T. Dickinson, Phys. Rev. Lett. **59**, 2795 (1987); J. Dickinson, S. Langford, L. Jensen, G. McVay, J. Kelso, and C. Pantano, J. Vac. Sci. Technol. A **6**, 1084 (1988); T. Miura and K. Nakayama, J. Appl. Phys. **88**, 5444 (2000).

[6] A. Gonzales and C. Pantano, Appl. Phys. Lett. **57**, 246 (1990).

[7] D. Bahat, V. Frid, A. Rabinovitch, and V. Palchik, Int. J. Fract. **116**, 179 (2002); A. Rabinovitch, D. Bahat, and D. Frid, Int. J. Rock Mech. Min. Sci. **39**, 125 (2002).

[8] V. Frid, A. Rabinovitch, and D. Bahat, Philos. Mag. Lett. **79**, 79 (1999).

[9] A. Rabinovitch, V. Frid, and D. Bahat, Phys. Rev. E **65**, 011401 (2001).

[10] C. Mavromatou, V. Hadjicontis, D. Ninos, D. Mastroyiannis, E. Hadjicontis, and K. Eftaxias, Phys. Chem. Earth, Part B **29**, 353 (2004).

[11] D. Bahat, A. Rabinovitch, and V. Frid, *Tensile Fracturing in Rocks* (Springer, New York, 2005).

[12] Y. Fujinawa and K. Takahashi, Phys. Earth Planet. Inter. **105**, 249 (1998).

[13] M. Hayakawa, *Atmospheric and Ionospheric Electromagnetic Phenomena Associated with Earthquakes* (Terrapub, Tokyo, 1999).

[14] M. Hayakawa and O. Molchanov, *Seismo Electromagnetics* (Terrapub, Tokyo, 2002).

[15] N. Gershenzon, and G. Bambakidis, Russ. J. Earth Sci. **3**, 247 (2001).

[16] K. Eftaxias, P. Kapiris, J. Polygiannakis, N. Bogris, J. Kopanas, G. Antonopoulos, A. Peratzakis, and V. Hadjicontis, Geophys. Res. Lett. **28**, 3321 (2001).

[17] K. Eftaxias, P. Kapiris, E. Dologlou, J. Kopanas, N. Bogris, G. Antonopoulos, A. Peratzakis, and V. Hadjicontis, Geophys. Res. Lett. **29**, 69/1 (2002).

[18] K. Eftaxias, P. Frangos, P. Kapiris, J. Polygiannakis, J. Kopanas, A. Peratzakis, P. Skountzos, and D. Jaggard, Fractals **12**, 243 (2004).

[19] Y. F. Contoyiannis, P. G. Kapiris, and K. A. Eftaxias, Phys. Rev. E **71**, 066123 (2005).

[20] P. G. Kapiris, K. A. Eftaxias, and T. L. Chelidze, Phys. Rev. Lett. **92**, 065702 (2004).

[21] Y. Contoyiannis, F. Diakonos, P. Kapiris, A. Peratzakis, and K. Eftaxias, Phys. Chem. Earth, Part B **29**, 397 (2004).

[22] P. Kapiris, J. Polygiannakis, X. Li, X. Yao, and K. Eftaxias, Europhys. Lett. **69**, 657 (2005).

[23] P. Kapiris, K. Nomicos, G. Antonopoulos, J. Polygiannakis, K. Karamanos, J. Kopanas, A. Zissos, A. Peratzakis, and K. Eftaxias, Earth, Planets Space **57**, 215 (2005).

[24] A. I. Khinchin, *Mathematical Foundations of Information Theory* (Dover, New York, 1957).

[25] J. S. Nicolis, *Chaos and Information Processing* (World Scientific, Singapore, 1991).

[26] G. Nicolis, *Introduction to Nonlinear Science* (Cambridge University Press, Cambridge, England, 1995).

[27] G. Nicolis and P. Gaspard, Chaos, Solitons Fractals **4**, 41 (1994).

[28] G. Nicolis, C. Nicolis, and J. S. Nicolis, J. Stat. Phys. **54**, 915 (1989).

[29] W. Ebeling and G. Nicolis, Chaos, Solitons Fractals **2**, 635 (1992).

[30] J. M. Borwein and K. Karamanos (unpublished).

[31] G. Nicolis, G. Rao, J. Rao, and C. Nicolis, in *Coherence and Chaos in Dynamical Systems*, edited by P. L. Christiansen and R. D. Parmentier (Manchester University Press, Manchester, England, 1988).

[32] W. B. EbelingR. Steuer, , and M. R. Titchener, Stochastics Dyn. **1**, 1 (2001); M. R. Titchener, in *International Symposium on Information Theory* (MIT, Boston, 1998); M. R. Titchener, in *IEEE Data Compression Conference* (Snowbird, Utah, 2000).

[33] R. Steuer, L. Molgedey, W. Ebeling, and M. A. Jimenez-Montano, Eur. Phys. J. B **19**, 265 (2001).

[34] S. Pincus, Proc. Natl. Acad. Sci. U.S.A. **88**, 2297 (1991).

[35] P. Grassberger and I. Procaccia, Phys. Rev. A **28**, 2591 (1983).

[36] S. Pincus and A. Goldberger, Am. J. Physiol. **266**, H1643 (1994); S. Pincus and B. Singer, Proc. Natl. Acad. Sci. U.S.A. **93**, 2083 (1996).

[37] C. Heneghan and G. McDarby, Phys. Rev. E **62**, 6103 (2000).

[38] B. Mandelbrot and J. Ness, SIAM (Soc. Ind. Appl. Math.) J. Numer. Anal. **10**, 422 (1968).

[39] A. Ponomarev, A. Zavyalov, V. Smirnov, and D. Lockner, Tectonophysics **277**, 57 (1997).

[40] D. Alexeev and P. Egorov, Reports of RAS **333**, 769 (in Russian) (1993).

[41] D. Alexeev, P. Egorov, and V. Ivanov, Physical-Technical Problems of Exploitation of Treasures of the Soil **5**, 27 (in Russian) (1993).

[42] X. Lei, K. Masuda, O. Nishizawa, L. Jouniaux, L. Liu, W. Ma, T. Satoh, and K. Kusunose, J. Struct. Geol. **26**, 247 (2004).

[43] H. Herrmann and S. Roux, *Statistical Models for Fracture of Disordered Media* (North-Holland, Amsterdam, 1990); C. Vanneste and D. Sornette, J. Phys. I **2**, 1621 (1992); L. Lamaignere, F. Carmona, and D. Sornette, Phys. Rev. Lett. **77**, 2738 (1996); J. V. Andersen, D. Sornette, and K. T. Leung, *ibid.* **78**, 2140 (1997); D. Sornette, *Critical Phenomena in Natural Sciences* (Springer, Berlin, 2000); T. Chelidze, Phys. Earth Planet. Inter. **28**, 93 (1982).

[44] A. Petri, G. Paparo, A. Vespignani, A. Alippi, and M. Costantini, Phys. Rev. Lett. **73**, 3423 (1994); A. Guarino, A. Garcimartin, and S. Ciliberto, Eur. Phys. J. B **6**, 13 (1998); A. Guarino, S. Ciliberto, A. Garcimartin, and M. Zei, *ibid.* **26**, 141 (2002); P. Diodati, F. Marchesoni, and S. Piazza, Phys. Rev. Lett. **67**, 2239 (1991).

[45] D. Sornette and C. Sammis, J. Phys. I **5**, 607 (1995); D. Bowman, G. Quillon, C. Sammis, A. Sornette, and D. Sornette, J. Geophys. Res. **103**, 24359 (1998).

[46] H. E. Stanley, Rev. Mod. Phys. **71**, 358 (1999); T. Vicsek, Nature (London) **418**, 131 (2002).

[47] J. Hopfield, Phys. Today **40** 40 (1994); A. Herz and J. Hopfield, Phys. Rev. Lett. **75**, 1222 (1995); J. B. Rundle, W. Klein, S. Gross, and D. L. Turcotte, Phys. Rev. Lett. **75**, 1658 (1995).

[48] D. Jaggard, in *Recent Advances in Electromagnetic Theory*, edited by H. Kritikos and D. Jaggard (Springer-Verlag, Berlin, 1990).

[49] X. Lei, O. Nishizawa, K. Kusunose, A. Cho, T. Satoh, and O. Nishizawa, Tectonophysics **328**, 329 (2000).

[50] H. Li, Z. Jia, Y. Bai, M. Xia, and F. Ke, Pure Appl. Geophys. **159**, 1933 (2002); B. Shaw, J. Carlson, and J. Langer, J. Geophys. Res. **97**, 479 (1992); D. Dodge, G. Beroza, and W. Ellsworth, *ibid.* **101**, 371 (1996); P. Reasenberg, Pure Appl. Geophys. **155**, 355 (1999).

[51] Z. Reches and D. Lockner, J. Geophys. Res. **99**, 159 (1994); D. Lockner and T. Madden, *ibid.* **96**, 643 (1991).

[52] C. Kontoes, P. Elias, O. Sycioti, P. Briole, D. Remy, M. Sachpazi, G. Veis, and I. Kotsis, Geophys. Res. Lett. **27**, 3989 (2000).

[53] A. Tzanis and K. Makropoulos, Natural Hazards **27**, 85 (2002).

[54] S. A. Pulinetes and K. Boyarchuk, *Ionospheric Precursors of Earthquakes* (Springer, Heidelberg, 2004); D. Ouzounov, S. Pulinets, N. Bryant, P. Taylor, and F. Freund, Geophys. Research Abstracts **7**, 05974 (2005); A. Tronin, M. Hayakawa, and O. Molchanov, J. Geodyn. **33**, 519 (2002); D. Ouzounov and F. Freund, Adv. Space Res. **33**, 268 (2004).

[55] C. Filizzola, N. Pergola, C. Pietrapertosa, and V. Tramutoli, Phys. Chem. Earth, Part B **29**, 517 (2004).

[56] A. Takeuchi, B. Lau, and F. T. Freund, Phys. Chem. Earth, Part B (special issue), (to be published); F. T. Freund, J. Keefner, J. J. Mellon, A. Lau, and D. Ouzounov, Geophysical Research Abstracts **7**, 09568 (2005).

[57] P. Varotsos, *The Physics of Seismic Electric Signals* (Terrapub, Tokyo, 2005); P. A. Varotsos, N. V. Sarlis, and E. S. Skordas, Phys. Rev. E **66**, 011902 (2002); **67**, 021109 (2003).

[58] P. Varotsos and K. Alexopoulos, *Thermodynamics of Point Defects and their Relation with Bulk Properties* (North-Holland, Amsterdam, 1986); P. Varotsos, M. Lazaridou, K. Eftaxias, G. Antonopoulos, J. Makris, and J. Kopanas, in *The Critical Review of VAN: Earthquake Prediction from Seismic Electric Signals*, edited by Sir J. Lighthill (World Scientific, Singapore, 1996), p. 29.

[59] P. Varotsos, K. Eftaxias, V. Hadjicontis, N. Bogris, E. Skordas, P. Kapiris, and M. Lazaridou, Acta Geophys. Pol. **XLVII**, 435 (1999).

[60] P. Bernard, P. Pinettes, P. Hadjidimitriou, E. Scordilis, G. Veis, and P. Milas, Geophys. J. Int. **131**, 467 (1997).

[61] S. Qian *et al.*, in *Electromagnetic Phenomena Related to Earthquake Prediction* (Terrapub, Tokyo, 1994), p. 205; D. Zhang *et al.*, in *Electromagnetic Phenomena Related to Earthquake Prediction* (Terrapub, Tokyo, 1994), p. 213.